TECHNICAL NOTE
D-1046

EXPERIMENTAL INVESTIGATION OF AN AIR-COOLED TURBINE

OPERATING IN A TURBOJET ENGINE AT TURBINE INLET

TEMPERATURES UP TO 2500° F

By Reeves P. Cochran and Robert P. Dengler

Lewis Research Center
Cleveland, Ohio

NATIONAL AERONAUTICS AND SPACE ADMINISTRATION

WASHINGTON   July 1961
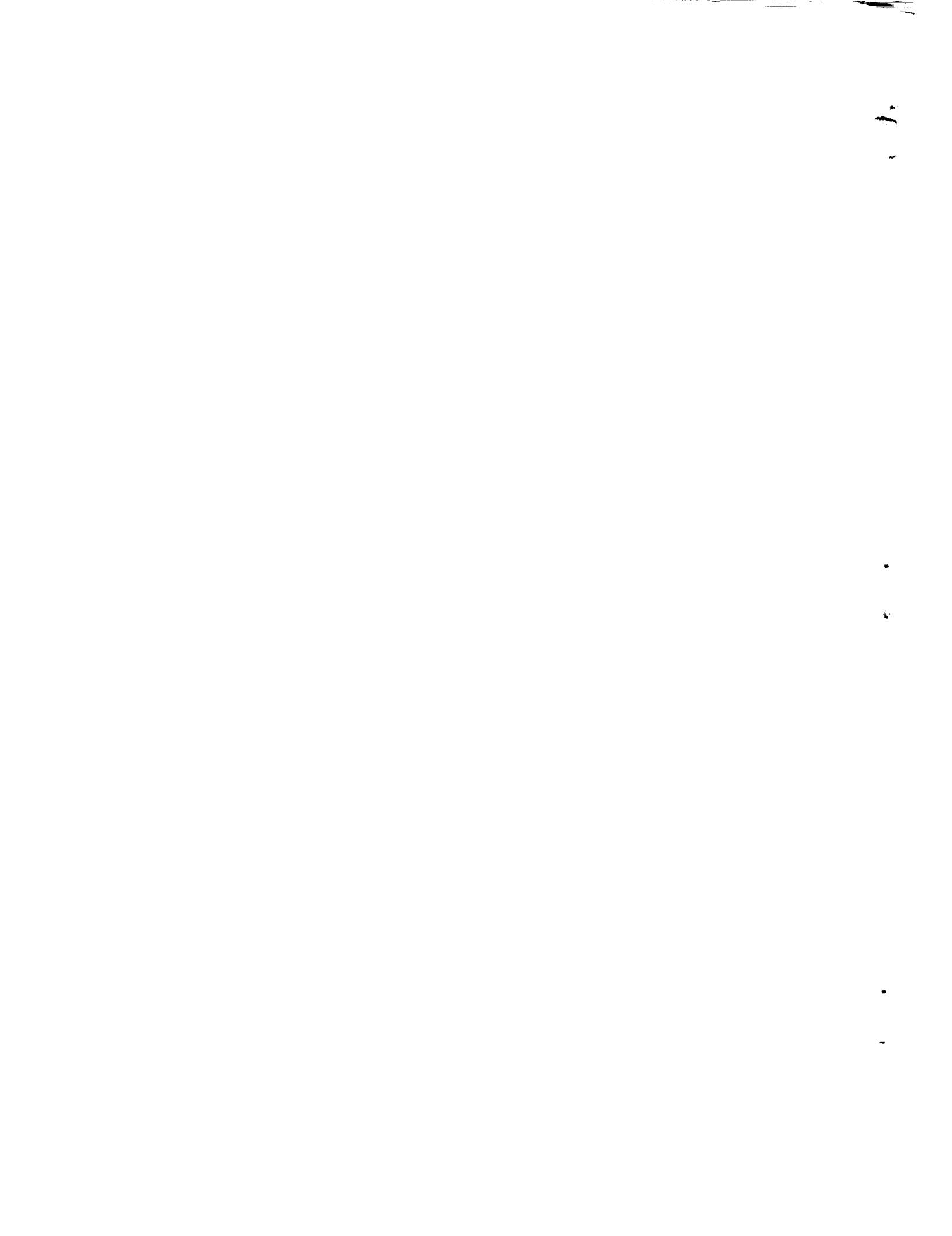
NATIONAL AERONAUTICS AND SPACE ADMINISTRATION

TECHNICAL NOTE D-1046

EXPERIMENTAL INVESTIGATION OF AN AIR-COOLED TURBINE OPERATING IN A

TURBOJET ENGINE AT TURBINE INLET TEMPERATURES UP TO 2500° F

By Reeves P. Cochran and Robert P. Dengler

SUMMARY

An experimental investigation was made of an air-cooled turbine at average turbine inlet tempertures up to 2500° F. A modified production-model 12-stage axial-flow-compressor turbojet engine operating in a static sea-level stand was used as the test vehicle. The modifications to the engine consisted of the substitution of special combustor and turbine assemblies and double-walled exhaust ducting for the standard parts of the engine. All of these special parts were air-cooled to withstand the high operating temperatures of the investigation.

The air-cooled turbine stator and rotor blades were of the corrugated-insert type. Leading-edge tip caps were installed on the rotor blades to improve leading-edge cooling by diverting the discharge of coolant to regions of lower gas pressure toward the trailing edge of the blade tip. Caps varying in length from 0.15- to 0.55-chord length were used in an attempt to determine the optimum cap length for this blade.

The engine was operated over a range of average turbine inlet temperatures from about 1600° to about 2500° F, and a range of average coolant-flow ratios of 0.012 to 0.065. Temperatures of the air-cooled turbine rotor blades were measured at all test conditions by the use of thermocouples and temperature-indicating paints. The results of the investigation indicated that this type of blade is feasible for operation in turbojet engines at the average turbine inlet temperatures and stress levels tested (maximums of 2500° F and 24,000 psi, respectively). An average one-third-span blade temperature of 1300° F could be maintained on 0.35-chord tip cap blades with an average coolant-flow ratio of about 0.022 when the average turbine inlet temperature was 2500° F and cooling-air temperature was about 260° F. All of the leading-edge tip cap lengths improved the cooling of the leading-edge region of the blades, particularly at low average coolant-flow ratios. At high gas temperatures, such parts as the turbine stator and the combustor liners are likely to be as critical as the turbine rotor blades.

INTRODUCTION

Significant increases in the power output of turbojet engines are made possible by utilizing turbine cooling to allow increased turbine inlet temperatures (ref. 1 to 3). In addition, increased turbine inlet temperatures offer improvements in specific fuel consumption for nearly all flight speeds of afterburning engines and for some supersonic applications of nonafterburning engines. To realize these potential gains requires turbine blading capable of withstanding the higher temperatures involved. Various types of convection-, film-, or transpiration-cooled blades using air as the coolant have been investigated by the NASA at present-day gas-temperature levels of 1600° to 1700° F (ref. 1). A type of air-cooled turbine rotor blade that showed promise of providing high cooling effectiveness at elevated temperatures was the shell-supported corrugated-insert blade (refs. 4 to 6). In addition, this type has the further advantages of light weight and relatively simple fabrication techniques. To obtain experimental data on this type of blade and other cooled components at higher gas temperatures, the present investigation was undertaken utilizing an air-cooled turbine in a turbojet engine operating at average turbine inlet temperatures up to 2500° F.

In general, the leading-edge section of the turbine blade is the most difficult portion to cool because of the high heat flux and the restricted space available for placing internal coolant passages at this location. Early attempts to improve the cooling of the leading-edge region with copper cladding on the inner surface of the shell (ref. 7) and with film-cooling of the immediate leading-edge area through spanwise slots (ref. 8) were not satisfactory. The first method reduced the structural integrity of the blade by increasing the stress level, and the second method subjected the blade to vibratory failure from the addition of the slots. However, the use of chordwise leading-edge tip caps to divert the discharge of coolant for the leading-edge passages to a lower-pressure region toward the rear of the blade chord has been shown in reference 9 to be effective at low coolant-flow rates.

This report presents the cooling characteristics of corrugated-insert blades of various tip cap lengths installed in a split-disk turbine rotor assembly and operated in a modified production-model turbojet engine at static sea-level conditions. A brief discussion of other engine components that may be critical when operated at high temperature levels is also presented. A detailed description of the special parts, modifications, and cooling-air systems required for this high-temperature engine are discussed in appendix A. The engine was operated at average turbine inlet temperatures from about 1600° to about 2500° F, and average turbine rotor blade coolant-flow ratios of 0.012 to 0.065.

APPARATUS AND INSTRUMENTATION

The test vehicle for this investigation was a modified production model of a 12-stage axial-flow-compressor turbojet engine (see fig. 1). The engine was installed and operated in a static sea-level test stand. The modifications to the engine consisted of air-cooled turbine rotor and stator assemblies (fig. 2), special combustors (figs. 3 and 4), and air-cooled double-walled exhaust ducting (figs. 1 and 2) in place of the standard engine parts. Blades for both the turbine stator and rotor assemblies were convection-cooled corrugated-insert type with corrugations of 0.07-inch pitch, 0.07-inch amplitude, and 0.007-inch thickness. Leading-edge tip caps of various lengths were added to the turbine rotor blades (figs. 5 and 6) to improve the cooling of the leading-edge section. Cooling air for the cooled components was supplied from a source external to the engine. Detailed descriptions of the design and fabrication of the special engine parts and the cooling-air systems are given in appendix A.

Temperatures of the air-cooled turbine rotor blades were measured by means of thermocouples (located as shown in fig. 7) and temperature-indicating paints. The details of the rotor blade instrumentation (as well as other instrumentation on the engine) are given in appendix A.

PROCEDURE

Experimental Procedure

The test engine was operated in a series of constant-engine-speed runs at progressively increasing levels of turbine inlet temperature. At each condition of speed and temperature, varying quantities of cooling airflow (beginning with high flows and decreasing to low flows) were supplied to the turbine rotor blades. The original test program provided for varying the supply of cooling air to the turbine stator blades also; but, because of mechanical damage to the blades, which was sustained early in the program and which will be described later, a constant high flow of cooling air was supplied to the stator blades throughout the tests as a precautionary measure. The coolant flows to the other cooled components (the turbine blade blowout shroud and the double-walled exhaust ducting) were approximately constant throughout the series of tests. Temperature, pressure, engine speed, and fuel-flow readings were made at each engine operating condition.

Calculation Procedure

Average turbine inlet temperature. - Because of the high operating temperatures proposed for this investigation, it was not practical to

measure turbine inlet temperature by the conventional means of mast-support thermocouples. As a consequence, an average turbine inlet temperature was calculated from measured conditions at the compressor discharge, measured quantity of fuel flow, and an assumed combustion efficiency. This method is outlined in detail in reference 10.

Rewriting equation (8) of reference 10 in terms used herein,

$$h_3 = \frac{\eta_B \overline{H} f + h_2 + f h_f}{(1 + f)} \tag{1}$$

All symbols are defined in appendix B. The burner efficiency η_B was assumed to be 98 percent (from experimental combustor data), and the lower heating value of the fuel $\overline{H}$ was determined experimentally to be 18,700 Btu per pound. With measured values of the compressor discharge temperature, the enthalpy at this station h_2 was determined from Chart I of reference 10. A constant value of -45 Btu per pound was used for the quantity h_f. From the calculated values of enthalpy at turbine inlet h_3, measured values of fuel-air ratio f, and Chart II of reference 10, the value of average turbine inlet temperature T_3 was determined.

Effective gas temperature. - The equilibrium temperature of an uncooled body in a gas stream is defined as the effective gas temperature $t_{g,e}$. It has a value between that of the static and total temperature of the gas. In previous turbine-cooling investigations conducted at lower turbine inlet temperature levels, it was possible to measure this temperature directly by use of thermocouples on an uncooled turbine blade installed in the rotor along with the cooled test blades. In the present investigation, however, the inlet temperatures were too high to permit operation of an uncooled blade; therefore, it was necessary to rely on calculated values of the effective gas temperature.

In order to calculate the rotor blade local effective gas temperature, it is necessary to know the turbine velocity diagram, the average radial gas-temperature distribution at the turbine inlet, and the heat loss to the stator blade cooling air. (The word "average" in the average radial gas-temperature distribution refers to a circumferential average temperature that the rotor blade "sees.") During high-temperature runs, it is extremely difficult to obtain adequate measurements of the gas-temperature distribution or the turbine velocity diagram. It was therefore necessary to resort to some assumptions that are believed to result in calculations of local effective gas temperature that are as accurate as can be obtained under the conditions of the test. These assumptions are given in appendix C. Using these assumptions, the local effective gas temperature at the radial position where the blade temperature measurements were made on the turbine rotor blade (one-third span) was calculated in the manner shown in appendix C.

Distribution of turbine rotor blade cooling air. - During this investigation, air-cooled turbine rotor blades with six different leading-edge tip cap configurations were tested simultaneously in the engine. The various tip caps had resulted in different internal airflow and discharge conditions that undoubtedly resulted in unequal coolant weight-flow rates. It was not possible to determine the flow of cooling air to each type of blade during engine operation. In the presentation of data, both average cooling-air to gas weight-flow ratio and cooling-air pressure level were used as criteria for evaluating cooling characteristics.

Where comparisons were made between blades of different tip cap configurations or for the uncapped blades, a measured average total pressure of the rotor blade cooling air (at the hub inlet near the shaft centerline) was used as the criterion. This method of comparison shows the relative cooling effectiveness of the various tip cap configurations where the conditions of cooling-air supply pressure and full-chord gas-stream pressure gradient and pressure level at the blade tips were the same. The quantity of cooling air flowing in the various types of blades would probably be different because of the different effective gas-stream pressure gradients developed by the presence of the tip caps. The magnitude of these differences in quantity of cooling airflow could not be measured during engine operation.

When comparisons were made between blades with 0.35-chord tip caps, an average coolant-flow ratio $\left(w_a/w_g\right)_{av}$ was used. This ratio was determined from the total quantity of cooling air for the rotor blades w_a and the combustion-gas weight flow w_g. From the breakdown of blade types listed in appendix A, it can be seen that the blade group with 0.35-chord tip cap comprised roughly one-third the total number of blades. If the two adjacent groups, which have very similar cooling-airflow characteristics, were added to this group, more than two-thirds of the blades would be represented, with the remainder evenly divided in categories above and below this central grouping. Therefore, the use of an average coolant-flow ratio for presenting the comparative cooling characteristics of the blades with a 0.35-chord tip cap should be a very good approximation of the actual cooling airflow to these blades.

RESULTS AND DISCUSSION

The operation of the air-cooled turbojet engine covered a range of average turbine inlet total temperatures from about 1600° to about 2500° F and a range of engine speeds from about 7000 to about 7650 rpm (approximately 88 to 96 percent of rated engine speed). Average cooling-air to combustion-gas weight-flow ratios (designated herein as average coolant-flow ratios) to the turbine rotor blades were varied from 0.012

to 0.065. A summary of the engine operation is given in table I. A total of about 19 hours of engine operating time was accrued during the course of this investigation. About six of these hours were at temperatures above 2000° F.

Turbine Rotor Blade Cooling Characteristics

The major effort in this investigation was devoted to determining the cooling characteristics of the turbine rotor blades. The use of convection-air-cooled blades with corrugated inserts in turbojet engines at turbine inlet temperatures up to 2500° F has been proposed in analytical studies (refs. 11 and 12). Some predictions of air-cooled turbine rotor blade temperatures at such elevated gas-temperature levels have also been made based on experimental blade temperature data obtained at conventional gas-temperature levels around 1600° F (see ref. 13). The present test apparatus afforded an opportunity experimentally to obtain temperature distributions on the turbine rotor blades, required quantities of coolant flow, and effects of rotor blade leading-edge tip caps under actual engine operating conditions at gas temperatures up to 2500° F. Results from the blades with 0.35-chord tip cap were used for most of the data presentation.

Chordwise blade temperature distribution. - The chordwise variation of outer-shell temperature at the one-third-span position on turbine rotor blades with 0.35-chord tip caps is shown in figure 8 for series C (table I). (Locations of the thermocouple positions plotted are shown on figure 7.) Series C was used to illustrate chordwise temperature variations because it covered a large range of average coolant-flow ratios and all of the blade thermocouples were operating properly. Other operating conditions for this series of runs were an average turbine inlet temperature of about 2000° F and an engine speed of 6970 rpm (88 percent of maximum engine speed).

The maximum chordwise spread in temperature for a given coolant-flow ratio was about 1000° F at the highest ratio (0.054). The temperature spread was about 800° F at the lowest coolant-flow ratio (0.013). This wide chordwise temperature spread was due to the extremely low local temperatures at the three-quarter-chord position on the suction surface and high peak temperatures at the leading edge. The high peak temperatures are confined to the leading-edge region, which represents about 10 percent of the blade chord, and the gradients in this region are very large.

For all thermocouple locations except in the leading region and at the trailing edge (suction surface), the change of the local temperature over this range of average coolant-flow ratios was 200° to 300° F. For the trailing-edge (suction-surface) region this change was about 150° F, and for the leading-edge region about 60° to 80° F.

It will be noted from the data shown in figure 8 and in table I that, in general, the temperature of the cooling air at the base of the turbine rotor blades t_a increased with decreases in average coolant-flow ratio w_a/w_g. This temperature increase was due to the fact that the cooling air absorbed heat in its passage through the impeller between the two halves of the split-type turbine rotor. With lower coolant flows, this heat addition resulted in higher temperature rises. The amount of this heat addition varied between series of runs because the heat input to the rotor disks increased with gas-temperature level.

Comparison of thermocouple and temperature-indicating-paint data. - The temperature-indicating paints were not used as primary sources of temperature data. However, the indications produced by these paints were useful in showing general trends of temperature variation. The sprayed coating of all the paints remained on the suction surfaces of the blades, but practically all the paint coatings were scrubbed off the pressure surface during engine operation. Therefore, data for the suction surface only will be presented for the temperature-indicating paints.

Figure 9 shows a composite diagram of the temperature patterns (isothermal lines) developed on rotor blades with 0.35-chord tip caps during the engine operation of series E. This series was used to illustrate the comparison between thermocouple and temperature-indicating-paint data, because all eight types of temperature-indicating paint had been used on the blades during this series. In addition, the gas-temperature level was high, and a large range of average coolant-flow ratios was covered. Maximum local temperatures registered by thermocouples during this same engine operation are superimposed on the figure for comparison. (Duplicate readings for a given thermocouple location are for two similar thermocouples on different blades.) In general, the agreement of data from the thermcouples and the temperature-indicating paints is very good. Five out of the six thermocouple readings are between isothermal lines bracketing the thermocouple readings. The other reading is slightly above the isothermal line that most nearly corresponds to it. The pattern of the isothermal lines verifies the existence of a low-temperature region at the three-quarter-chord suction surface, which was indicated by the thermocouple readings as shown in figure 8. The patterns developed on blades with other tip cap lengths were of similar appearance, and the comparison with corresponding thermocouple readings in general showed about the same agreement exhibited by the example shown in figure 9.

Effect of leading-edge tip caps on blade temperature. - Leading-edge tip caps of varying lengths had been installed on the blades to improve the cooling of the leading-edge regions. These caps would shield the tip end of the leading-edge coolant passages from the high pressure

of the gas stream at the turbine inlet and divert the discharge of cool-
ant to a location of lower gas pressure closer to the turbine exit. To
be of real value, any gain in cooling of the leading-edge region due to
the tip caps must be made without undue penalty to the cooling effective-
ness of the remainder of the blade.

Local turbine rotor blade temperatures at the leading-edge, mid-
chord section (suction-surface), and trailing-edge positions for blades
with various lengths of tip caps are shown in figure 10 for engine op-
erating series C (table I). Series C was used for this comparison be-
cause more temperature data were obtained on more tip cap configurations
in this series than in any other. This series also covered a large av-
erage coolant-flow-ratio range. Temperature trends for the other series
were similar to the ones shown here. All the thermocouples for a given
type of capped blade are located on the same blade (except that a du-
plicate thermocouple was located at the midchord suction-surface posi-
tion on a second blade with a 0.35-chord tip cap). Data for the 0.15-
chord tip cap blade are not included on this figure because of faulty
thermocouples on this blade. Temperature readings for the blade with
0.45-chord tip cap looked questionable during the test. This blade was
subsequently sectioned, and blocked cooling-air passages were discovered.
Hence, these data were omitted. Coolant-flow rates to each of the dif-
ferent types of blades were not known; therefore, the temperature data
on figure 10 are plotted against the rotor hub cooling-air pressure P_a,
which was the same for all blades. The corresponding values of average
coolant-flow ratio for the data points are also given on the figure.

The temperatures measured on the leading edge of the uncapped blade
(fig. 10(a)) were higher than those measured on the leading edge of any
of the capped blades for the entire range of rotor hub cooling-air pres-
sures. It can also be seen that for the capped blades the leading-edge
temperatures did not vary greatly with the cooling-air pressure. For
the uncapped blade, the leading-edge temperature increased 125° F from
about 1615° F at a cooling-air pressure of 54 inches of mercury to about
1740° F at 33 inches of mercury. For the same range of cooling-air
pressure the leading-edge temperatures of the capped blades increased
only about 35° F. At the high values of cooling-air pressure the
uncapped-blade leading-edge temperature was slightly higher than that of
the blades having 0.25- and 0.55-chord tip caps and about 50° F higher
than the blade with a 0.35-chord tip cap. At the low cooling-air pres-
sures, however, the uncapped-blade leading-edge temperature is 100° to
150° F higher than that of the capped blades. This indicates that the
tip caps are more effective at the low cooling-air pressures (low cool-
ant flows) than at the high cooling-air pressures, which is a desirable
result.

It will be noted that there is a dashed-line curve for the uncapped-
blade leading-edge temperature for cooling-air pressures less than about

38 inches of mercury. It is believed that this curve more nearly represents the trend of the leading-edge temperature for the uncapped blade than does the solid-line curve for the low cooling-air pressures. The basis for this belief is discussed in appendix D in conjunction with the determination of effective gas temperatures.

The temperature patterns at the trailing edge (fig. 10(c)) are very similar to those at the leading edge with some interchanging of the relative positions of the curves for the capped blades. The uncapped blade showed slightly higher temperatures at this position also than any of the capped blades.

At the midchord position, the spread in temperatures is much larger both with changes in tip cap length and with changes in cooling-air pressure (fig. 10(b)). Here, also, the effect of the tip caps can be seen at the lower pressure levels. The midchord temperatures of the uncapped and the shortest capped blades show sharp increases as the cooling-air pressure is reduced below about 38 inches of mercury, while the temperatures of the longer capped blades are still increasing gradually.

It was not possible to establish the optimum cap length from the data obtained, but is obvious that the tip caps were beneficial. The indications are that cap lengths of 0.35-chord and possibly 0.55-chord length were the most effective. The improved cooling of the capped blades is significant in that the lower leading-edge temperatures can mean less erosion of the metal and higher permissible stresses (greater mass flow for given engine size). Although the temperature differences are not great, even moderate temperature reductions can have appreciable effects on material properties at high temperatures. It can be concluded that leading-edge tip caps were helpful additions to the air-cooled turbine rotor blades.

Required turbine rotor blade average coolant-flow ratio. - Average blade temperatures for 0.35-chord tip cap blades were determined by integrating the areas under the curves of chordwise temperature distribution (as in fig. 8) for all the operating conditions. These average blade temperatures (which are listed in table I) were plotted against the corresponding average coolant-flow ratios with average turbine inlet temperature as a parameter. This information was then cross-plotted to obtain figure 11, which is a plot of required average coolant-flow ratio for various average turbine inlet temperatures and average blade temperatures.

It can be seen from figure 11 that an average coolant-flow ratio of 0.022 will maintain an average blade temperature of 1300° F at an average turbine inlet temperature of 2500° F. At an average turbine inlet temperature of 2140° F, this same average blade temperature can be maintained with an average coolant-flow ratio of about 0.01. (The cooling-air temperatures for these conditions were about 260° F for the high gas-temperature level, and 350° F for the low gas-temperature level.) Since

this is a relatively low-stress blade (24,000 psi maximum at root section), an average blade operating temperature of 1300° F is not excessive. It has been shown in reference 14 that the stress-ratio factor (ratio of average allowable blade stress-rupture strength to blade average centrifugal stress at the critical section) was a good design criterion for tube-filled air-cooled blades. From reference 15, the stress-rupture strength of the blade material (HS-31) at 1300° F for 100-hour life is 46,000 psi. The critical section on an air-cooled rotor blade is generally near the one-third-span position. At that span position on this blade, the centrifugal stress was a maximum of 18,800 psi during this investigation. This resulted in a stress-ratio factor of 2.45. The experimental endurance investigation of reference 16 has shown that a value of stress-ratio factor of 2.3 was a good design value for a tube-filled air-cooled blade cast of a low-alloy steel.

Temperature-difference ratio. - The temperature-difference ratio $(t_{g,e} - t_{b,av})/(t_{g,e} - t_a)$ was derived in reference 17 to express the one-dimensional radial average blade temperature distribution for an air-cooled turbine blade. The temperature $t_{g,e}$ was calculated by the method given in appendix C; $t_{b,av}$ was determined by integrating under the curves of chordwise temperature distribution such as shown in figure 8; t_a was measured at the base of the turbine rotor blades. A tabulation of these values is given in table I.

The assumption is sometimes made that the value of the temperature-difference ratio remains constant (or at least does not decrease appreciably) when the engine operating temperature level is increased. The results of the present investigation (which covers a turbine inlet temperature range from 1620° to 2520° F) show that this assumption would lead to predicted blade temperatures that were higher than would occur in actual operation. A plot of temperature-difference ratio against coolant-flow ratio for 0.35-chord tip cap blades is shown in figure 12. As can be seen from this figure, the value of the temperature-difference ratio at a given value of coolant-flow ratio increased with an increase in average turbine inlet temperature.

The reader is reminded that certain assumptions (listed in appendix C) were made in calculating the $t_{g,e}$ values used to determine the temperature-difference ratios shown in figure 12. In making these assumptions it is more likely that the calculated values of $t_{g,e}$ are low rather than high. It is therefore possible that the values of temperature-difference ratios appearing in figure 12 are also low. The trend of temperature-difference ratio with turbine inlet temperature shown was obtained from one engine. It should not be treated as a general result applicable to all types of engines and turbine blading without

due regard to these qualifying assumptions. It is felt, however, that the evidence of this trend for this investigation is of interest to those concerned with the design of air-cooled turbojet engines.

Effects of High-Temperature Operations on Engine Parts

All parts of the engine from the combustors rearward were subjected to the effects of the high gas temperature. Where possible, air-cooling was applied to these parts to protect them from failure due to the temperature effects. The success of this air-cooling was dependent on a number of factors such as rate of heat input and accessibility of the part for cooling.

Combustors. - The modified combustors used in this investigation had been subjected to the conditions of high-temperature engine operation (part of which is reported in ref. 6) before being employed in this engine. This previous service covered 7 hours or more at turbine inlet temperatures between 1800° and 2500° F. No damage was apparent to the combustors at the conclusion of this service; therefore, the same units were used in the engine for the present investigation.

At the conclusion of the experimental operation summarized in table I, the combustor transition liners showed considerable damage due to the high-temperature effects. Two views of a typical liner after testing are shown in figure 13. The inner radius of the liner showed more damage than the outer radius, because the line of flow of the combustion gas leaving the combustor impinged on this section.

The combustors were modifications of an existing design for a production-model engine rather than a design specifically made for the high temperature proposed for this investigation. The exposed position of the cooling-air scallops on the transition liners made them particularly susceptible to damage from gas-stream impingement. The present experience shows, however, that limited high-temperature operation was possible with modified combustors in which only a small amount of development work was conducted. An original design that has better radial and circumferential temperature distribution and avoids exposed surfaces in the gas flow could undoubtedly be developed to give much better service.

Air-cooled stator assembly. - Early in the test program a piece of debris (a small part of a broken machine screw tap that had inadvertently been left in such a position that it could go through the turbine) caused severe damage to the trailing-edge section of the stator blades and moderate damage to the leading-edge section of the rotor blades. The last inch and a half of the trailing edge of every stator blade was struck repeatedly on the suction surface by the debris. In all of these places

the outer shell on the suction surface was bent in, sealing off the cooling passages underneath. Some of the blows were hard enough to bulge and crack the pressure surface directly opposite the point of impact, also. No replacement parts were available for the stator blades; therefore, repairs were made by straightening and welding where possible. The tests were continued, with a large amount of cooling air being supplied constantly to the stator to help overcome the effect of the badly blocked internal cooling-air passages in the trailing edge of the blades. The condition of the forward part of the stator assembly at the conclusion of the investigation is shown in figure 14. This is a view of a sector of the stator diaphragm directly behind the discharge of one of the eight can-type combustors. The hot core of the gas stream is plainly defined by the damage pattern on the blades. The most severe damage is from the midspan outward. The coloration pattern on the stator blades that is evident in figure 14 shows that the stator blade cooling air (with possibly some assistance from the transition-liner cooling air) was keeping the root end of the blades very cool. This pattern of blade damage was similar behind each of the other combustors. The inner and outer rings of the stator diaphragm and the inlet and exit cooling-air manifolds that composed the remainder of the stator assembly showed no signs of damage from high-temperature engine operation.

The condition of the stator blades clearly shows the necessity of controlling the temperature distribution at the exit of the combustors for high-temperature engines. The blades had been cooled with a high rate of coolant flow (5 to 8 percent) throughout the investigation because of the damage to the trailing-edge section early in the program. This cooling was adequate for all except the extreme leading-edge section, where the high stagnation temperature of the gas stream is felt. The gas temperature at the midspan was well above the average calculated turbine inlet temperature listed in table I. The use of properly designed annular combustors with reduced temperature gradients in the gas stream probably would reduce greatly the cooling problem for the leading edge of the stator blades.

Air-cooled turbine rotor assembly. - During the course of the investigation two failures of turbine rotor blades occurred. Neither of these failures was due to basic deficiencies in the cooling abilities of the blades. The first blade failure was due to the mechanical damage sustained by the leading-edge portion of the blade from the passage of the same debris that severely damaged the stator blades. A crack originating in one of the damage marks resulted in the failure in the outer half of the blade for a distance roughly 1/2 inch back from the leading edge. The second failure was due to the loss of the inner-shell cap at the base of the blade (fig. 5). The braze joint holding this cap to the inner shell failed, and the cap was thrown out the tip of the blade. The cooling air then flowed through the inner passage of the inner shell rather than through the corrugated cooling passages, and the blade failed

at midspan from insufficient cooling. Subsequent visual inspection of the other rotor blades revealed several similar braze-joint cracks.

Some local erosion of the outer shell of the turbine rotor blades was evident in a small area at the leading edge outboard of the half-span position. The amount of erosion was not severe at the end of the present test program, but long-term service at high temperatures may show more serious erosion damage.

With the exception of the points noted, the rotor blades were in good condition at the end of the investigation. Since the materials used to make these blades were not necessarily the same as would be chosen for a production engine, any statement about the condition of these blades can only be interpreted as an indication of the cooling effectiveness of the blade design. From this point of view, the present design has been shown to be adequate for the operating conditions investigated.

The split-disk rotor with the internal sheet-metal cooling-air impeller performed satisfactorily with respect to both cooling and mechanical operation.

Air-cooled exhaust ducting. - This special exhaust ducting was a research tool to permit operation of the engine at the high temperatures, but no attempt was made in its original design to provide for highly effective cooling. It is felt that more efficiently cooled exhaust ducting can be designed with available heat-transfer data. Total coolant-flow rates of between 2.5 and 4 pounds per second of low-pressure air were supplied to the exhaust ducting during the course of the investigation. Some local warpage of the inner walls of the ducting was observed at the conclusion of the test, but in general the cooling of the double-walled ducting was very effective. At the flange connections where the parts of exhaust ducting joined and the double-walled construction was interrupted, the metal parts were a cherry-red during operation. Except for isolated hot spots, the outer wall of the ducting was below the dull-red range (about 1000° F) at all times.

SUMMARY OF RESULTS

The following results were obtained in an experimental investigation of a modified turbojet engine operated under static sea-level conditions at high turbine inlet temperatures:

1. Convection-air-cooled turbine rotor blades with corrugated inserts appear to be feasible for operation in turbojet engines at average turbine inlet temperatures up to 2500° F and a root stress of about

24,000 psi. The average blade temperature at the one-third-span location could be maintained at 1300° F with an expenditure of about 1 percent of the engine mass flow for rotor blade coolant when the average turbine inlet temperature was 2140° F and cooling-air temperature about 350° F. For an average turbine inlet temperature of 2500° F, a coolant flow of approximately 2.2 percent of the engine flow would be required. An average blade temperature of 1300° F would result in a stress-ratio factor (allowable to actual stress) of about 2.45 at the critical one-third-span location.

2. Turbine rotor blade leading-edge tip caps (which divert the discharge of cooling air for the leading-edge coolant passages to a point of lower pressure) improved the cooling of the leading-edge region particularly at low average coolant-flow ratios (0.02 or less). Data obtained were not conclusive enough to make a definite selection of the optimum tip cap length, but the indications were that the longest cap (0.55 chord) resulted in the lowest average blade temperature.

3. The value of the temperature-difference ratio increased with gas-temperature level. Thus, extrapolation of blade temperature data on the assumption that the temperature-difference ratio is constant with increasing gas-temperature level is likely to give higher values of blade temperature than would actually occur.

4. In addition to the turbine rotor blades, other critical parts in a high-temperature turbojet engine are likely to be the aft end of the combustion chambers and the turbine stator blades. These parts are subjected to high heat fluxes and often to extreme variations in temperatures because of the combustion profiles. Minimizing temperature gradients at combustor discharge will be extremely important at high operating temperatures.

5. Although damage did occur to the combustors and to the turbine stator and rotor blades of this experimental engine that is attributable to high-temperature operation, the results of this investigation indicate that air-cooled gas-turbine engines can be designed for operation at average turbine inlet temperatures up to at least 2500° F.

Lewis Research Center
    National Aeronautics and Space Administration
        Cleveland, Ohio, June 1, 1961

APPENDIX A

DESCRIPTION OF SPECIAL PARTS, COOLING-AIR

SYSTEMS, AND INSTRUMENTATION

The special parts, the cooling-air systems, and the instrumentation that were used on the experimental engine to permit operation at turbine inlet temperatures up to 2500° F are described in the following paragraphs.

Air-Cooled Turbine Rotor Blades

A cutaway drawing of the air-cooled, corrugated-insert turbine rotor blade is shown in figure 5.

Aerodynamic design. - The aerodynamic design of the air-cooled turbine rotor blade was based on modifications to the profile of the standard turbine rotor blade for the test engine. These modifications were made for the purpose of simplifying the problem of cooling the blades. The trailing-edge section of a turbine rotor blade is normally long and thin to reduce blade aerodynamic losses. However, such sections are difficult to cool. Therefore, in the air-cooled blade design, a relatively thick trailing edge was employed in order to allow more space for coolant passages. The thick trailing edge will increase the aerodynamic losses relative to the standard blade unless the ratio of the trailing-edge thickness to pitch is held constant (ref. 18). This suggests a reduction in the number of blades. To maintain the same blade solidity, an increase in the axial chord of the blade was also required. A change in the number of rotor blades from 96 to 72 was chosen for this design. The blade solidity at the tip section of the cooled turbine was maintained at the same value as that for the standard turbine by increasing the tip chord length of the standard blade by a factor of 1.333 (or 96/72) to obtain the chord length for the cooled blade. Some further increase in the periphery of the cooled blade tip section was necessary to provide sufficient space for all of the corrugated coolant passages. This was accomplished by retaining the mean camber line corresponding to the new blade chord length and making small changes in the blade profile (increasing suction-surface camber and decreasing pressure-surface camber). To avoid having an excessively long axial chord at the blade root section with an accompanying long blade base and wide turbine rotor, the blade chord at this section was only slightly increased, resulting in a lower blade solidity at this position than that of the standard engine. A multiplier factor of 1.176 was used to convert the standard blade root chord length to the new chord length. This lower solidity at the root section resulted in a blade with very little change in the chord length

over the blade span, which greatly aided the placement of the corrugated
cooling passages around the periphery of the blade profile. Other span-
wise sections of the blade were determined by a straight-line fairing
between the tip and root sections. The resulting aerodynamic profiles
were checked for surface velocity variations by a stream-filament-theory
procedure outlined in reference 19.

Heat transfer and mechanical design. - Previous analytical and
experimental studies have shown that the use of internal fins made of a
continuous corrugated sheet is a promising way to augment the cooling
surface of an air-cooled blade. The addition of an inner shell (as in
fig. 5) makes more efficient use of the cooling air by restricting the
flow to the vicinity of the exposed outer shell where the heat load is
and also increases the flow velocity of the air. From a structural
standpoint, the corrugations and inner shell add rigidity to the thin
outer shell. References 4 to 6 show the cooling results of experimental
investigations with different sizes of corrugated inserts. Reference 20
gives a method for designing corrugated surfaces for effective cooling
of air-cooled turbine rotor blades. The geometry of the insert chosen
for this blade on the basis of effective cooling and ease of fabrication
consisted of corrugations with 0.07-inch pitch, 0.07-inch amplitude, and
0.007-inch thickness. An inner-shell thickness of 0.01 inch and a ta-
pered outer shell varying in thickness from 0.06 at the root to 0.03
inch at the tip was used for this blade. This combination of outer
shell, corrugations, and inner shell resulted in a centrifugal stress
at the blade root of about 25,000 psi at rated engine speed (7954 rpm).

The use of leading-edge tip caps to divert the discharge of cooling
air from the passages in the leading edge to a region of lower pressure
closer to the turbine exit has been shown in reference 9 to be a prom-
ising way of improving leading-edge cooling for this type of blade.
Diversion of the coolant discharge in this manner increases the total-
pressure head available to force air through the passages sheltered from
the high-pressure gas stream by the tip cap. This increase in pressure
head means greater flow rates and therefore better cooling. Blade tip
caps of 15, 25, 35, 45, and 55 percent of chord length (fig. 6) were
used in an attempt to determine the optimum cap length for this blade.
Uncapped blades were also included for comparison purposes. The number
of blades of each configuration installed in the rotor were as follows:

Tip-cap length Chord length	Number of blades
0	2
.15	8
.25	18
.35	25
.45	9
.55	10
Total	72

To provide space for the diverted air to flow under the cap for transfer to the discharge point at the rear end of the cap, the tips of the corrugations and the inner shell were cut back as shown on figure 5. A uniform angle of 25° (between axial direction and line of cut on insert) was used at the forward part of the cutback on all blades. This angled cut extended to a point directly under the rear edge of the tip cap. The bottom of the cutback was parallel to the tip cap and extended from 1/16 to 3/16 inch depending on the length of the tip cap. The rear part of the cutback was at a uniform angle of 45° for all blades.

The two-serration base for this blade shown in figure 5 is taken from a design presented in reference 21. The geometry of the cooling-air passage in the base changes from a rectangular shape at the inlet to an airfoil shape that matches the inner profile of the blade outer shell. The transverse bulkhead in the center of the base is for the purpose of resisting collapsing loads due to the tangential component of centrifugal force on the blade and compressive rim stresses due to radial thermal gradients in the rotor disks.

Fabrication. - As a fabrication expedient, the outer shell and base of the blade were precision-cast (by the lost-wax method) of a high-temperature alloy (HS-31). All corrugated-insert blades previously referenced in this report have consisted of cast or forged bases and sheet-metal shells and fins joined by brazing and/or welding. This latter method of fabrication should result in a better turbine rotor blade than the casting method that was used. However, fabrication facilities for utilizing this method were not available at the time the hardware was being made. To simplify the placing of the insert within the blade, the blade casting was made in two pieces with parting lines at the leading and trailing edges from the blade tip to the bottom of the blade base. The corrugations (0.007 in. thick) and inner shell (0.010 in. thick) were each formed in two pieces of HS-25 high-temperature alloy to fit the pressure and suction surfaces of the blade. Cutbacks were made on the corrugations and the inner shell to match the length of tip cap for the blade. A base cap of 0.03-inch HS-25 was used to seal the lower end of the inner shell.

The parts for the rotor blade were assembled by first brazing the halves of the corrugated insert and the inner shell to the corresponding casting of half the blade outer shell and base. The brazing alloy (wire form Nicrobraz 30) was inserted in the corrugated passages. Heavy metal brazing fixtures were used to ensure good contact of parts during brazing and to prevent distortion of the brazed assembly. Following this brazing operation, the base cap for the inner shell was tack-welded to the suction-surface half of the blade, and the two halves of the blade were then heliarc-welded at the leading and trailing edges of the airfoil and the base. Heavy copper welding fixtures were used to hold the blade halves for welding and to conduct heat away from the welding zone while maintaining the proper airfoil shape. Braze material was then placed

inside the leading and trailing edges of the inner shell, on the inner-shell base cap, and on the parting lines of the blade castings inside the base. A "U"-shaped strip (which extended about 1.5 in. down from the blade tip) was coated with braze material and placed between the blade halves near the trailing edge (see fig. 6) to stiffen this part of the blade. The assembly was put through a second braze cycle, again using heavy metal brazing fixtures to maintain contact of parts and to prevent distortion during brazing. All brazing operations on the rotor blades were conducted in a vacuum furnace. Following the second braze cycle, serrations were ground on the blade base, and the base was subsequently machined to the proper axial length. The blade tips were then ground to the required length, and the leading-edge tip caps of proper length were heliarc-welded in place. The tip caps were made from 0.02-inch-thick HS-25 sheet material.

Endurance testing of turbine rotor blades. - Four turbine rotor blades were subjected to an endurance test in another engine for periods up to 101 hours and at one-third-span blade temperature of 1350° F. The blades were not cooled during this test. The endurance test approximately duplicated the centrifugal-stress level throughout the blade and the one-third-span blade temperature of the final engine operation. Aerodynamic conditions of the gas stream and the temperature variations within the cooled blades could not be duplicated in this test. Since the major stress in the rotor blade is centrifugal rather than bending due to the gas loads, the differences in aerodynamic forces between the endurance tests and final engine operation were not thought to be significant. The absence of large temperature variations within the blades because they were uncooled is hard to evaluate. Such temperature variations can introduce thermal stresses that may be appreciable

One of the four uncooled test blades failed in the valley of the top serration on the suction side after 101 hours of endurance testing. A second blade was cracked in this same location at the end of the same test period. The other two blades were tested for only 54 hours, and one of them was cracked in the serrations at the end of testing. A region of thin cross section existed at this point where the cooling-air passage inside the blade base came close to the serrations. To avoid a failure in this region in the final blades, the cross-sectional dimension of the blade casting was increased by adding metal on the inside surface. No further endurance testing was done after this change to the blade casting, but it was felt that the weak spot had been eliminated. The remainder of the blade was in excellent shape at the end of the endurance test.

Twenty heating and cooling cycles (starts and stops) were covered during the course of the endurance tests. This is a small number of cycles compared with what might be required of a blade in actual engine service. Cyclic-endurance testing of other types of air-cooled blades made of noncritical materials (ref. 14) showed that such blades withstood

over 100 cycles and final failure was due to severe oxidation. The material of this blade (HS-31) had better high-temperature properties than the material of the blade of reference 14 (Timken 17-22A(S), a low-alloy steel with 97-percent iron content), but the operating temperature level was higher for the HS-31 blade.

Air-Cooled Turbine Rotor

Various designs for air-cooled turbine rotor disks are presented in reference 21. The choice of the design for an engine application would depend, of course, on the specification for that particular engine. The design most adaptable to the engine that would be modified for this investigation was the split-disk type with forward-face entry of the cooling air. A cross-sectional view of this rotor is shown in figure 2. A complete description of the design analysis is given in reference 21. The halves of the air-cooled turbine rotor were machined from turbine rotor forgings for the production-model engine. The materials for these forgings were an SAE 4340 shaft and hub section and a Timken 16-25-6 rim. The two parts had been welded together at a radius of 10.75 inches. The rear disk was integral with the turbine rotor shaft. The forward disk had a central hole that permitted it to be slipped over the turbine shaft. The two disks were held together by 24 bolts equally spaced on a 9.5-inch radius. The inner faces of the two disks were machined to receive a sheet-metal impeller with 72 radial passages, which directed the cooling air to each of the 72 rotor blades. The disk bolts passed through the vanes of the impeller (between the radial cooling-air passages) and did not interfere with the cooling airflow. Blade base mounting serrations were broached with the halves of the disk bolted together.

Air-Cooled Turbine Stator

Stator blades. - As in the case of the turbine rotor blades, changes to the profile of the stator blades were made to improve the cooling of the blades. The changes to the stator blades were much less extensive than to the rotor blades. The same number of stator blades (64) was used in the air-cooled stator diaphragm as in the uncooled standard engine stator diaphragm. However, it was necessary to increase the trailing-edge radius from 0.016 to 0.035 inch to provide cooling-air passages for trailing-edge section of the blade. The blockage of the gas-flow channels caused by this thicker trailing edge was overcome by changing the angle of the stator blades 1° to open up the throat area at the stator exit.

A corrugated insert with the same pitch, amplitude, and thickness (0.07, 0.07, and 0.007 in., respectively) as the insert for the rotor blades was used for the stator blades. The outer shell of the stator

blade was formed from a single 0.02-inch-thick piece that was folded on a radial line at the leading edge. The corrugated insert was made in two pieces, one piece for the pressure surface and one piece for the suction surface. In like manner, the inner shell was formed in two pieces from 0.01-inch material. Inner-shell caps (also 0.01 in. thick) at both the inner and outer radii restricted the flow of cooling air to the corrugated passages. The space enclosed by the inner shell was vented by a hole in the cap at the outer radius. All parts of the stator blade were made of N-155 sheet stock.

The parts of the inner shell and the corrugations were fitted inside the outer shell, and the outer shell was then heliarc-welded along the trailing edge. Nicrobraz 30 in wire form was placed in the corrugated passages and inside the leading and trailing edges of the inner shell. The end caps for the inner shell were then tack-welded in place, and sufficient braze material was placed on the joint line between inner shell and cap to ensure a good bond. The assembly was furnace-brazed in a dry hydrogen atmosphere.

Stator assembly. - Figure 2 shows the air-cooled stator assembly in the engine. The inner and outer rings of the air-cooled stator diaphragm were made of stainless steel. Sixty-four contoured slots were machined through each ring to receive the blades. The outer shells of the blades protruded through both the inner and outer rings of the diaphragm by about 1/8 inch. These protrusions of the outer shells were heliarc-welded to both rings around the entire periphery of the blade profiles. Eight equally space sawcuts through the outer ring allowed for thermal expansion of the assembly. Sixteen 1-inch-diameter tubes ducted the cooling air to an inlet manifold on the inner radius of the air-cooled stator diaphragm. The cooling air flowed radially outward through the corrugated passages in the blades to an exit collection manifold encircling the outer periphery of the stator diaphragm.

Modified Combustors

The special combustors used in this investigation were modifications of the standard combustors for this engine. Cross-sectional drawings of the modified and unmodified combustors are shown in figure 3. A pictorial comparison of the transition liners is presented in figure 4. The modifications made to the combustion system were for the purpose of providing a larger flow of secondary (cooling) air over the outer surfaces of the sheet-metal parts of the system. The diameters of the circular aft end of the combustor liner, the combustor-outlet ring, and the forward end of the transition liner (fig. 3) were reduced so that a larger annular passage was provided through which secondary air could flow over the outer surfaces of the sheet-metal parts. The scalloped edge on the outer radius at the aft end of the transition liner was cut more deeply

and scallops were added to the aft edge at the inner radius to provide a larger exit path for the increased flow of secondary air. A sheet-metal shroud was built around the transition liner to direct the secondary air over the outer surface of the liner. The support struts of the unmodified version (fig. 4) were removed to prevent possible damage to the rotor and stator in case of failure of these struts during high-temperature operation. A complete description of the combustor modification and an experimental investigation of the modified combustor are given in reference 22.

Air-Cooled Exhaust Ducting

The proposed average turbine inlet temperature level of 2500° F would involve engine exhaust temperatures on the order of 2100° F. This temperature level is beyond the safe limit for the materials of the exhaust ducting, if the exposed surface was also the load-bearing structure. Therefore, a double-walled convective-cooled ducting with the outer wall as the structural member and the inner wall serving only as a boundary for the gas stream was used for most of the exhaust system.

Double-walled ducting. - All of the exhaust ducting aft of the turbine rotor blowout shroud (with the exception of the jet-nozzle section) was of double-walled construction (see fig. 1). Spacing between the inner and outer walls of the double-walled ducting was 1/4 inch. The combustion-gas-flow area of the air-cooled exhaust ducting was the same as that for the standard engine ducting. Material for the exhaust ducting was L-605 (HS-25) high-temperature alloy. The ducting was made in two sections. The foremost section was the tailcone, which included a 6-inch annular extension just behind the turbine rotor. This extension was added to provide better locations for pressure and temperature instrumentation at the turbine discharge. The inner cone, the outer cone, and the tailcone struts (which position the inner cone) were all of double-walled construction for air-cooling. This entire tailcone section was about 3 feet in axial length. The second section (tailpipe) was 7 feet long. Cooling air was supplied to annular inlet manifolds on the inner and outer cones of the tailcone and on the tailpipe. From these manifolds, air flowed parallel to the gas stream (counterflow in the case of the outer cone) between the inner and outer ducting walls. Air for cooling the tailcone struts was introduced along the leading edge of the strut and flowed rearward between the two walls to the trailing edge. Cooling air from the outer cone of the tailcone and from the tailpipe was collected in annular manifolds for subsequent discharge to a location outside the test facility. Cooling air from the inner cone and the struts of the tailcone discharged into the gas stream.

Turbine rotor blade blowout shroud. - A thin (0.043-in.) Inconel blowout shroud surrounded the turbine rotor to allow any sizable part of a failed blade to escape by piercing the shroud. This shroud was fitted

inside an axial spacer that was inserted between the engine proper and the tailcone (fig. 2). Part of the weight of the exhaust ducting was carried by this spacer, which is a framework of two flanges separated by 24 axial rods. The forward flange is bolted to the stator cooling-air exit manifold, and the rear flange is bolted to the tailcone. Cooling air was directed over the outer surface of the blowout shroud from circumferential rings mounted on the two flanges of the spacer.

Cooling-Air Systems

Any cooling system for an aircraft must be a self-contained unit. For an air-cooling system where pressurized air is required, the logical source of such air is the engine compressor - either at compressor discharge or interstage, depending on the pressure level required. Where low-pressure air will suffice as the cooling medium, ram air is a readily available source. For this investigation, these two normal cooling-air sources were simulated by laboratory room-temperature air sources. Use of these laboratory air sources permitted wide variation in the pressures and flow rates of the coolant. The pressure and quantity of flow were regulated to each of the cooled components independently by appropriate pressure regulators and flow-control valves.

Room-temperature laboratory air at pressures within the limits of compressor discharge pressure (up to 150 in. Hg abs) was supplied to the turbine rotor and stator blades. Use of this low-temperature external air in place of compressor discharge air (at temperature of 450° to 500° F) simulated the existence of an intercooler in the cooling-air system between compressor discharge and the cooled parts. If compressor discharge air were used without some intercooling, a larger airflow rate would be required to effect the same amount of cooling.

All parts of the exhaust ducting (including the turbine blade blowout shroud) were cooled with room-temperature laboratory air at pressures of about 1.25 to 1.5 atmospheres (sea level). For an aircraft in subsonic flight, these conditions would simulate the conditions of ram air used for cooling.

Instrumentation

Engine. - All pressure readings were measured on manometer tubes that were mounted on a large board and photographed during engine operation for subsequent manual interpretation. The temperature readings from the thermocouples were recorded on an automatic digital potentiometer. Pressure and temperature levels were measured at engine station 2 (fig. 1). The engine mass flow was measured by means of a Venturi tube that supplied ambient air to the test cell in which the engine was

mounted. The cooling-air mass flows to the turbine rotor and stator blades and to the various parts of the double-walled exhaust ducting were measured by means of sharp-edged orifices. Engine fuel flow was measured with a vane-type magnetic-impulse flowmeter, and engine speed was measured with a magnetic-impulse speed counter.

Turbine rotor. - Temperatures on the outer shell of the turbine rotor blades were measured by means of Chromel-Alumel thermocouples located at various chordwise positions at a distance of 1.25 inches from the top of the blade base platform, as shown in figure 7. Thermocouples of the same alloy were used to measure the temperature of the cooling air in the front and rear parts of the blade base. Only blades with 35-percent-chord-length tip caps had thermocouples in all the positions shown on figure 7. Because of the limited capacity of the rotating slip-ring pickup, the greatest number of thermocouples were concentrated on this type of blade with a medium tip cap length. The outer-shell thermocouples were cemented into radial grooves milled in the shell. A complete description of this method of thermocouple installation is given in reference 23. The leads for the thermocouple extended from the thermocouple bead radially inward within the milled groove to the blade base, then rearward along the top of the base platform and radially inward on the back side of the turbine disk to terminal posts located on a 12-inch-diameter ring bolted to the rear disk (fig. 2). Extension leads ran from this point through a drilled passage on the centerline of the turbine shaft bolt and the compressor shaft to a slip-ring-type thermocouple pickup mounted on the front of the engine (fig. 1). The stationary part of this pickup was connected to the temperature-recording equipment.

In addition to the thermocouples, temperature-indicating paints were used to indicate maximum temperatures reached over the surface of the blade. Eight different temperature-indicating paints ranging in ratings from 824° to 2012° F were used in this investigation. The entire surface of a blade was sprayed with one type of paint. A total of about 38 blades covering six tip cap configurations were spray-coated. It has been shown in reference 23 that, to obtain effective temperature distributions with such paints under conditions encountered in jet-engine operation, the time of exposure should be limited to about 15 minutes. Because of the engine operating schedule for this investigation and the mechanical complications involved in installing and removing the air-cooled exhaust ducting, it was not practical to inspect the paint coatings this often. As a consequence, the patterns that were evident at the rather infrequent times of visual inspection were not the best temperature-indicating patterns that could have been developed if primary emphasis had been placed on the use of the paints. The paints were therefore treated as a secondary method of measuring blade temperatures.

Chromel-Alumel thermocouples were installed at several radial positions on the outer faces of both the front and rear halves of the turbine rotor for the purpose of monitoring the rotor temperatures.

APPENDIX B

SYMBOLS

A_R effective turbine rotor throat area

A_S effective turbine stator throat area

a_{cr} critical velocity relative to the stator, ft/sec

c_p specific heat at constant pressure, Btu/(lb)(°F)

f   fuel-air ratio

g   standard acceleration of gravity, ft/sec^2

$\overline{H}$ lower heating value, Btu/lb

h   enthalpy, Btu/lb

J   mechanical equivalent of heat, 778 ft-lb/Btu

LE   leading edge

N   engine speed, rpm

P_a total pressure of cooling air at rotor hub, in. Hg abs

R   gas constant, ft-lb/(lb)(°F)

T   average total gas temperature, °R unless otherwise specified

T'   average total gas temperature relative to the rotor, °R unless otherwise specified

TE   trailing edge

t   average static gas temperature, °R unless otherwise specified

t_a average cooling-air temperature at rotor blade base, °F

t_b local blade temperature, °F

$t_{b,av}$ average blade temperature for 1/3-blade-span position, °F

$t_{g,e}$ effective gas temperature at rotor inlet for 1/3-blade-span position, °F

U	blade velocity, ft/sec	
V	absolute gas velocity at rotor inlet,	$\sqrt{\gamma g R \left(\dfrac{2}{\gamma + 1}\right) T_3}$, ft/sec
V'	relative gas velocity at rotor inlet,	$\sqrt{V^2 + U^2 - 2UV \cos \beta_4}$, ft/sec
w_a	cooling airflow rate, lb/sec	
w_g	combustion gas-flow rate, lb/sec	
$\left(\dfrac{w_a}{w_g}\right)_{av}$	average coolant-flow ratio	
β_4	flow angle of absolute velocity of gas at stator exit measured from tangential direction, deg	
γ	ratio of specific heats	
η_B	combustor efficiency	
Λ	recovery factor	

Subscripts:

f	fuel
z	axial component
θ	tangential component
1	compressor inlet
2	compressor discharge
3	turbine stator inlet
4	turbine rotor inlet
5	turbine rotor discharge
6	tailpipe
7	jet nozzle

APPENDIX C

EFFECTIVE-GAS-TEMPERATURE CALCULATION PROCEDURE

FOR TURBINE ROTOR BLADES

The following assumptions were made in the calculation of the turbine rotor blade effective gas temperature $t_{g,e}$ at the one-third-span position:

(1) The flow was choked in both the stator and rotor throats. This assumption was made because this turbine approaches limiting loading and because small variations from choked flow would not appreciably affect the results.

(2) The mass flow is constant through the turbine stage. This assumption neglects the cooling air added to the exhaust gas from the rotor blades. Since this cooling air does no work and does not mix appreciably with the exhaust gas in passing through the rotor blading, its effect (if it were considered) would be only to reduce the effective area of the rotor throat available for the passage of the exhaust gas.

(3) The gas flow from the stator throat to the rotor throat was assumed to be at constant entropy.

(4) The average turbine inlet temperature T_3 could be calculated from measured conditions at the compressor discharge and measured fuel-flow rate as previously discussed in the PROCEDURE section. Because of the heat rejected to the stator blade cooling air in the passage of the exhaust gas through the stator diaphragm, it was necessary to correct the calulated average turbine inlet temperature T_3 to obtain the temperature conditions that existed at the entrance to the turbine rotor T_4. The amount of this correction was between 20° and 35° F for the engine conditions covered in the investigation.

(5) The stagnation state of the gas flow relative to a blade row remains constant from the entrance to the exit of the blade row.

(6) The effective stator-to-rotor throat area ratio A_S/A_R was constant over the range of engine operating conditions. Under the assumptions of these calculations, this ratio can be expressed as a function of $t_{g,e}$ (eqs. (C12) and (C13)). Making the further assumption that a close approximation of $t_{g,e}$ could be obtained from measured leading-edge temperatures of the uncapped blades at very low cooling airflows to the rotor blade (see appendix D), the value of this area ratio was determined from experimental data of the present investigation.

(7) The local recovery factor Λ had a value of 0.89 (ref. 24), and the stator discharge flow angle β_4 remained constant at 21°.

It will be advantageous to define a number of thermodynamic relations at the inlet to the turbine rotor. Symbols are defined in appendix B.

Effective gas temperature (nonrotating parts):

$$t_{g,e} \equiv t_4 + \Lambda \, (T - t)_4 \tag{C1}$$

Effective gas temperature (rotating parts):

$$t_{g,e} \equiv t_4 + \Lambda \, (T' - t)_4 \tag{C2}$$

Absolute stagnation temperature:

$$\left. \begin{aligned} T_4 &\equiv t_4 + \frac{V^2}{2gJc_p} \\ &\equiv t_4 + \frac{V^2(\gamma - 1)}{2\gamma gR} \end{aligned} \right\} \tag{C3}$$

Relative stagnation temperature:

$$\left. \begin{aligned} T_4' &\equiv t_4 + \frac{(V')^2}{2gJc_p} \\ &\equiv t_4 + \frac{(V')^2(\gamma - 1)}{2\gamma gR} \end{aligned} \right\} \tag{C4}$$

From turbine velocity triangle,

$$V^2 = V_z^2 + V_\theta^2 \tag{C5}$$

$$(V')^2 = V_z^2 + (V_\theta - U)^2 \tag{C6}$$

$$V_\theta = V \cos \beta_4 \tag{C7}$$

Absolute critical velocity:

$$a_{cr} = \sqrt{\frac{2\gamma}{\gamma + 1} \, gRT_4} \tag{C8}$$

Combining equations (C3), (C7), and (C8) results in

$$\left(\frac{t}{T}\right)_4 = 1 - \frac{\gamma - 1}{\gamma + 1} \left(\frac{V_\theta}{\cos \beta_4 \, a_{cr}}\right)^2 \tag{C9}$$

Equations (C3) to (C6) and (C8) can be combined to give

$$\left(\frac{T'}{T}\right)_4 = 1 - \frac{\gamma - 1}{\gamma + 1} \frac{U}{a_{cr}} \left(2 \frac{V_\theta}{a_{cr}} - \frac{U}{a_{cr}}\right) \tag{C10}$$

From assumptions (1) to (4) the temperature ratio $(T'/T)_4$ can be related also to the stator-to-rotor effective throat area ratio. The development of this relationship is covered in detail in reference 25. When expressed in the nomenclature of this report, this relationship (eq. (6), ref. 25) becomes

$$\frac{A_S}{A_R} = \left(\frac{T'}{T}\right)_4^{\frac{\gamma+1}{2(\gamma-1)}} \tag{C11}$$

Combining equations (C10) and (C11) gives

$$\frac{V_\theta}{a_{cr}} = \frac{1}{2}\left\{\frac{U}{a_{cr}} + \frac{\gamma+1}{\gamma-1}\frac{a_{cr}}{U}\left[1 - \left(\frac{A_S}{A_R}\right)^{\frac{2(\gamma-1)}{\gamma+1}}\right]\right\} \tag{C12}$$

Dividing equation (C2) by T_3 and combining with equations (C9) and (C10) give

$$\frac{t_{g,e}}{T_4} = \left[1 - \frac{1}{\cos^2\beta_4}\left(\frac{V_\theta}{a_{cr}}\right)^2\frac{\gamma-1}{\gamma+1}\right](1 - \Lambda) + \Lambda\left[1 - \frac{\gamma-1}{\gamma+1}\frac{U}{a_{cr}}\left(2\frac{V_\theta}{a_{cr}} - \frac{U}{a_{cr}}\right)\right] \tag{C13}$$

Values of $t_{g,e}$ for all engine operating points were calculated from equation (C13) by making use of assumptions (5) and (6) and equation (C12).

E-1163

APPENDIX D

DETERMINATION OF APPROXIMATE EFFECTIVE GAS TEMPERATURE FROM

UNCAPPED-BLADE LEADING-EDGE TEMPERATURE

Figure 15 shows the temperature of the leading edge of the uncapped turbine rotor blade plotted against the pressure of the cooling air measured at the rotor hub for series D. Because the quantity of cooling air was regulated by a throttling valve upstream of the blades, reductions in cooling-airflow rates meant lower cooling-air pressures. At very low average coolant-flow ratios (low cooling-air pressures), the temperature of the leading edge of the uncapped blade remained constant with further reduction in cooling airflow or lowering of cooling-air pressure level.

At pressures below about 39 inches of mercury absolute (fig. 15), the temperature of the leading edge was constant at about 1835° F for the conditions of this series of runs. This trend indicated that at these levels of cooling-air pressure the leading edge was uncooled because the pressure at the base of the blade was not sufficient to force coolant through the leading-edge passages against the high pressure existing in the gas stream at the leading edge of the blade tip. The general trend of the curve in figure 15 is representative of the behavior of the uncapped-blade leading-edge temperature at very low coolant flow for other engine operating conditions. The existence of this condition during engine operation justified the assumption made in appendix C (assumption (6)) for calculating effective gas temperature $t_{g,e}$.

REFERENCES

1. Esgar, Jack B.: Turbine Cooling. Jour. Eng. for Power, ser. A, vol. 81, no. 3, July 1959, pp. 226-233.

2. Weatherwax, W. F.: Design and Development of a Convective Air-Cooled Turbine and Test Facility. Jour. Eng. for Power, ser. A, vol. 83, no. 1, Jan. 1961, pp. 9-17; discussion, pp. 17-18.

3. Esgar, Jack B., and Ziemer, Robert R.: Effect of Turbine Cooling with Compressor Air Bleed on Gas-Turbine Engine Performance. NACA RM E54L20, 1955.

4. Bartoo, Edward R., and Clure, John L.: Experimental Investigation of Air-Cooled Turbine Blades in Turbojet Engine. XII - Cooling Effectiveness of a Blade with an Insert and with Fins Made of a Continuous Corrugated Sheet. NACA RM E52F24, 1952.

30

5. Cochran, Reeves P., and Dengler, Robert P.: Static Sea-Level Perform-ance of an Axial-Flow-Compressor Turbojet Engine with an Air-Cooled Turbine. NACA RM E54L28a, 1955.

6. Slone, Henry O., Cochran, Reeves P., and Dengler, Robert P.: Experi-mental Investigation of Air-Cooled Turbire Rotor Blade Temperatures in a Turbojet Engine Operating at Turbine-Inlet Temperatures up to 2850° R and Altitudes of 50,000 and 60,000 Feet. NACA RM E56C26, 1956.

7. Arne, Vernon L., and Esgar, Jack B.: Experimental Investigation of Air-Cooled Turbine Blades in Turbojet Engine. VI - Conduction and Film Cooling of Leading and Trailing Edges of Rotor Blades. NACA RM E51C29, 1951.

8. Ellerbrock, Herman H., Jr., Zalabak, Charles F., and Smith, Gordon T.: Experimental Investigation of Air-Cooled Turbine Rotor Blades in Turbojet Engine. IV - Effects of Special Leading- and Trailing-Edge Modifications on Blade Temperature. NACA RM E51A19, 1951.

9. Calvert, Howard F., Meyer, André J., Jr., and Morgan, William C.: Air-Cooled Turbine Blades with Tip Cap for Improved Leading-Edge Cooling. NASA MEMO 2-9-59E, 1959.

10. English, Robert E., and Wachtl, William W.: Charts of Thermodynamic Properties of Air and Combustion Products from 300° to 3500° R. NACA TN 2071, 1950.

11. Ziemer, Robert R., and Slone, Henry O.: Aralysis of Cooling-Air Requirements of Corrugated-Insert-Type Turbine Blades Suitable for a Supersonic Turbojet Engine. NACA RM E56B17, 1956.

12. Slone, Henry O., and Hubbartt, James E.: Analysis of Factors Affect-ing Selection and Design of Air-Cooled Single-Stage Turbines for Turbojet Engines. IV - Coolant-Flow Requirements and Performance of Engines Using Air-Cooled Corrugated-Irsert Blades. NACA RM E55C09, 1955.

13. Ellerbrock, Herman H., Jr., and Stepka, Francis S.: Experimental In-vestigation of Air-Cooled Turbine Blades in Turbojet Engine. I - Rotor Blades with 10 Tubes in Cooling-Air Passages. NACA RM E50I04, 1950.

14. Esgar, Jack B., and Clure, John L.: Experimental Investigation of Air-Cooled Turbine Blades in Turbojet Engine. X - Endurance Eval-uation of Several Tube-Filled Rotor Blades. NACA RM E52B13, 1952.

15. Anon.: Haynes Alloys for High-Temperature Service. Haynes Stellite Co., c. 1949-50.

E-1163

16. Stepka, Francis S., Bear, H. Robert, and Clure, John L.: Experimental Investigation of Air-Cooled Turbine Blades in Turbojet Engine. XIV - Endurance Evaluation of Shell-Supported Turbine Rotor Blades Made of Timken 17-22A(S) Steel. NACA RM E54F23a, 1954.

17. Livingood, John N. B., and Brown, W. Byron: Analysis of Spanwise Temperature Distribution in Three Types of Air-Cooled Turbine Blades. NACA Rep. 994, 1950. (Supersedes NACA RM'S E7B11e and E7G30.)

18. Heaton, Thomas R., Slivka, William R., and Westra, Leonard F.: Cold-Air Investigation of a Turbine with Nontwisted Rotor Blades Suitable for Air Cooling. NACA RM E52A25, 1952.

19. Hubbartt, James E., and Schum, Eugene F.: Average Outside-Surface Heat-Transfer Coefficients and Velocity Distributions for Heated and Cooled Impulse Turbine Blades in Static Cascades. NACA RM E50L20, 1951.

20. Slone, Henry O., Hubbartt, James E., and Arne, Vernon L.: Method of Designing Corrugated Surfaces Having Maximum Cooling Effectiveness Within Pressure-Drop Limitations for Application to Cooled Turbine Blades. NACA RM E54H20, 1954.

21. Moseson, Merland L., Krasner, Morton H., and Ziemer, Robert R.: Mechanical Design Analysis of Several Noncritical Air-Cooled Turbine Disks and a Corrugated-Insert Air-Cooled Turbine Rotor Blade. NACA RM E53E21, 1953.

22. Friedman, Robert, and Zettle, Eugene V.: Modified Tubular Combustors as High-Temperature Gas Generators. NACA RM E55H25, 1955.

23. Stepka, Francis S., and Hickel, Robert O.: Methods for Measuring Temperatures of Thin-Walled Gas-Turbine Blades. NACA RM E56G17, 1956.

24. Esgar, Jack B., and Lea, Alfred L.: Determination and Use of The Local Recovery Factor for Calculating the Effective Gas Temperature for Turbine Blades. NACA RM E51G10, 1951.

25. English, Robert E., and Cavicchi, Richard H.: One-Dimensional Analysis of Choked-Flow Turbines. NACA Rep. 1127, 1953. (Supersedes NACA TN 2810.)

E-1163

TABLE I. - SUMMARY OF TEST DATA

| Series	Run	Engine speed, N, rpm	Average turbine inlet temp., T_3, °F	Effective gas temp., $t_{g,e}$, °F	Average blade temp., $t_{b,av}$, °F	Cooling-air temp., t_a, °F	Average coolant-flow ratio, $(w_a/w_g)_{av}$	Coolant-flow rate, w_a, lb/sec	Rotor hub cooling-air pressure, P_a, in. Hg abs
A	1	6966	1839	1587	896	115	0.061	4.57	58.0
	2	6976	1760	1515	903	116	.047	3.55	48.7
	3	6965	1717	1476	944	150	.032	2.41	37.3
	4	6974	1650	1416	982	195	.020	1.54	33.0
	5	6975	1617	1386	1015	235	.015	1.16	30.2
B	6	7379	1956	1694	919	100	0.061	4.92	61.7
	7	7348	2019	1751	942	100	.061	4.88	61.4
	8	7343	2006	1739	967	110	.050	4.00	53.3
	9	7314	1996	1730	1045	144	.035	2.82	44.0
C	10	6978	2006	1737	985	91	0.054	4.07	54.5
	11	6968	2014	1744	1047	120	.039	2.90	44.8
	12	6966	2023	1751	1115	183	.024	1.8	37.5
	13	6972	2012	1741	1208	294	.013	.98	33.0
D	14	7645	2141	1863	1015	150	0.056	5.07	64.6
	15	7643	2140	1861	1055	164	.048	4.07	55.9
	16	7643	2142	1864	1075	178	.037	3.25	49.7
	17	7650	2144	1865	1127	195	.031	2.74	48.1
	18	7645	2151	1871	1225	267	.018	1.59	38.1
	19	7646	2145	1866	1300	353	.012	1.03	35.4
E	20	7310	2377	2074	1095	136	0.051	4.23	59.0
	21	7440	2380	2078	1117	139	.043	3.63	53.9
	22	7420	2389	2085	1172	168	.033	2.75	47.5
	23	7426	2418	2084	1226	206	.026	2.17	43.5
F	24	7448	2481	2169	1094	128	0.065	5.23	67.3
	25	7348	2498	2182	1116	122	.056	4.46	60.5
	26	7343	2513	2194	1149	134	.050	3.88	55.5
	27	7338	2522	2203	1195	154	.040	3.15	49.9
	28	7330	2520	2199	1257	219	.026	2.00	41.7
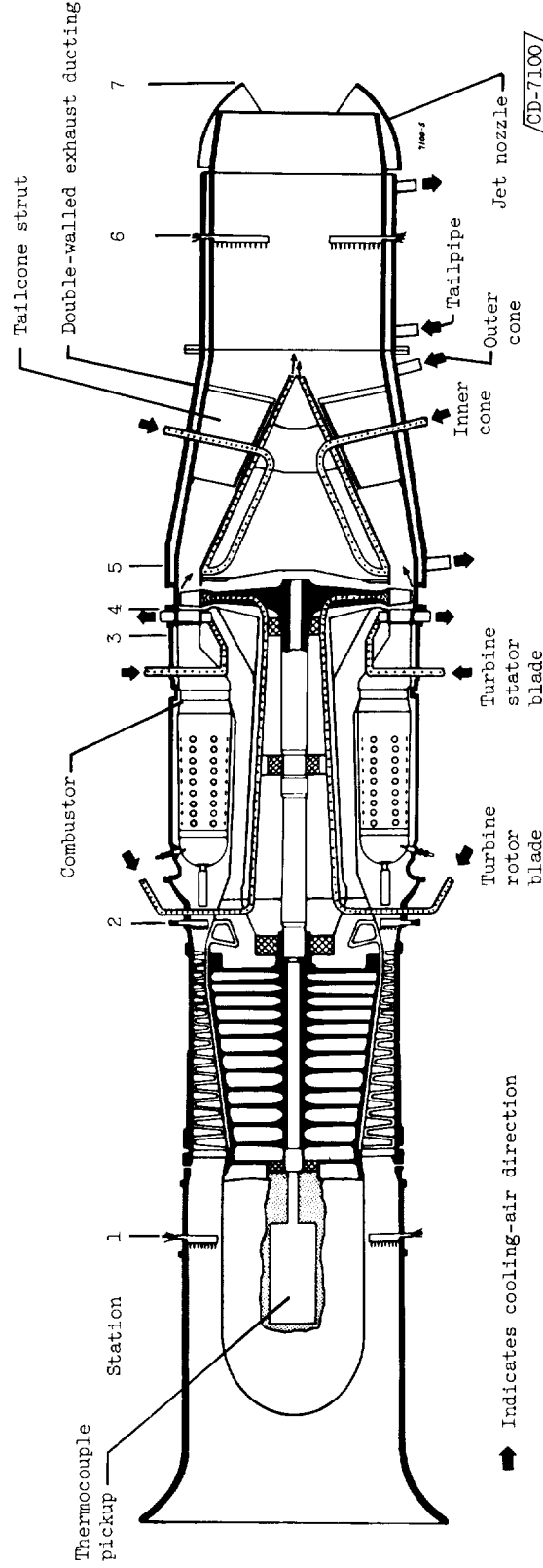
E-1163

Figure 1. - Schematic diagram of production-model axial-flow-compressor engine modified for turbine cooling.

Scalloped edges

Support struts
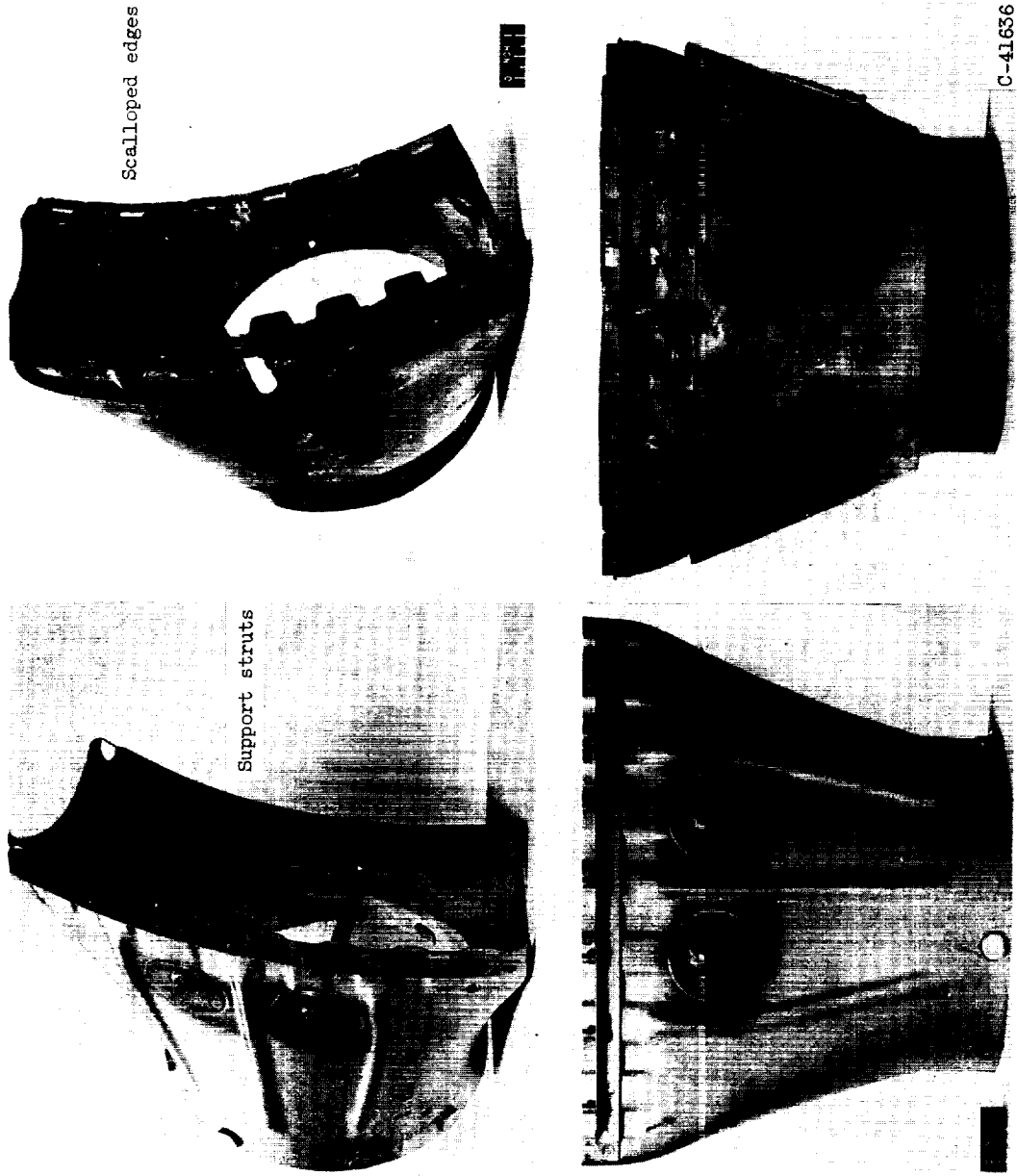
(a) Unmodified liner.

(b) Modified liner.

C-41636

Figure 4. - Modified and unmodified production-model combustor transition liners.

E-1163
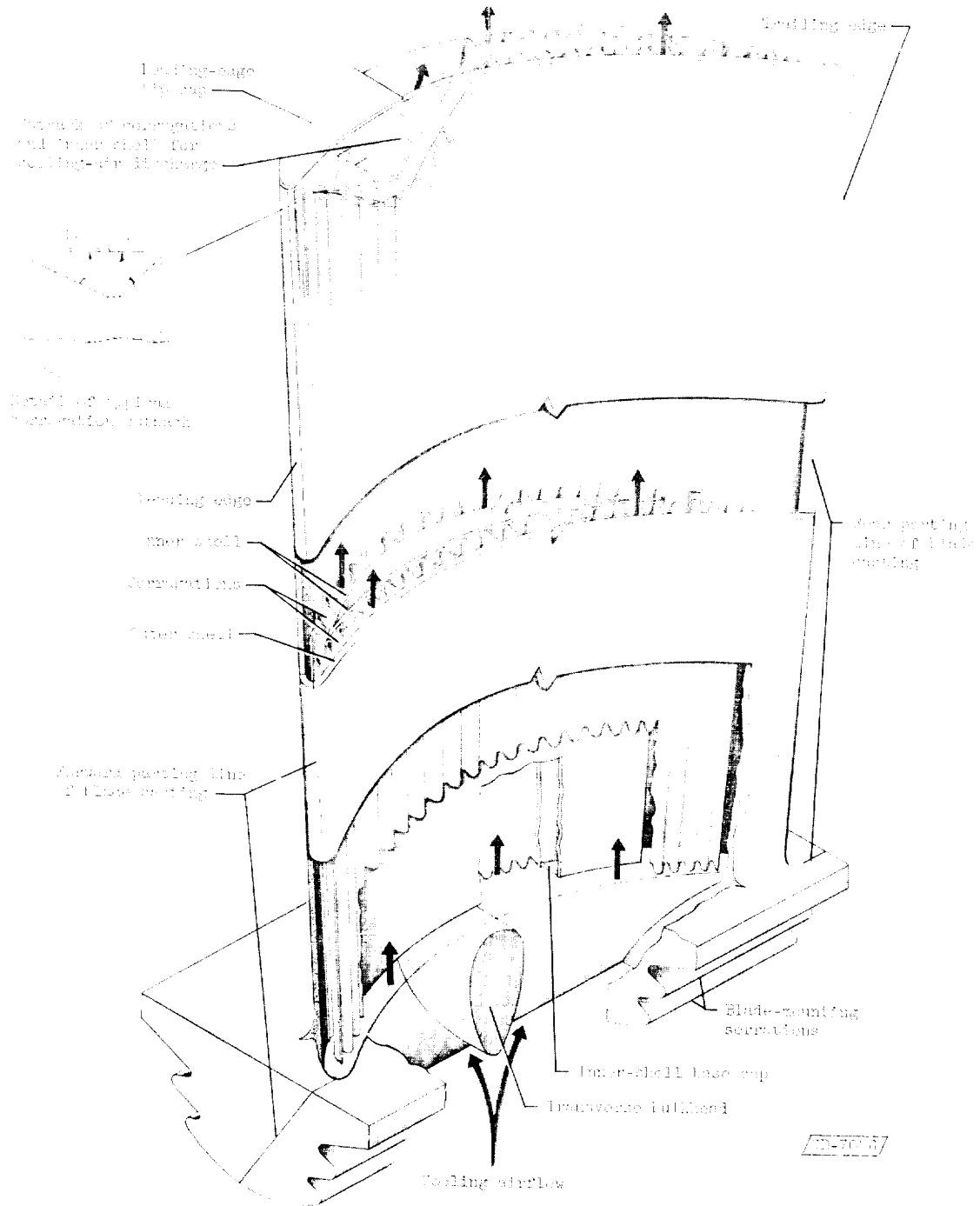
E-1163

Figure 5. - Cutaway view of air-cooled corrugated-insert turbine rotor blade
with leading-edge tip cap.

"U" channel

C-47554

0 INCH

0   .15   .25   .35   .45   .55
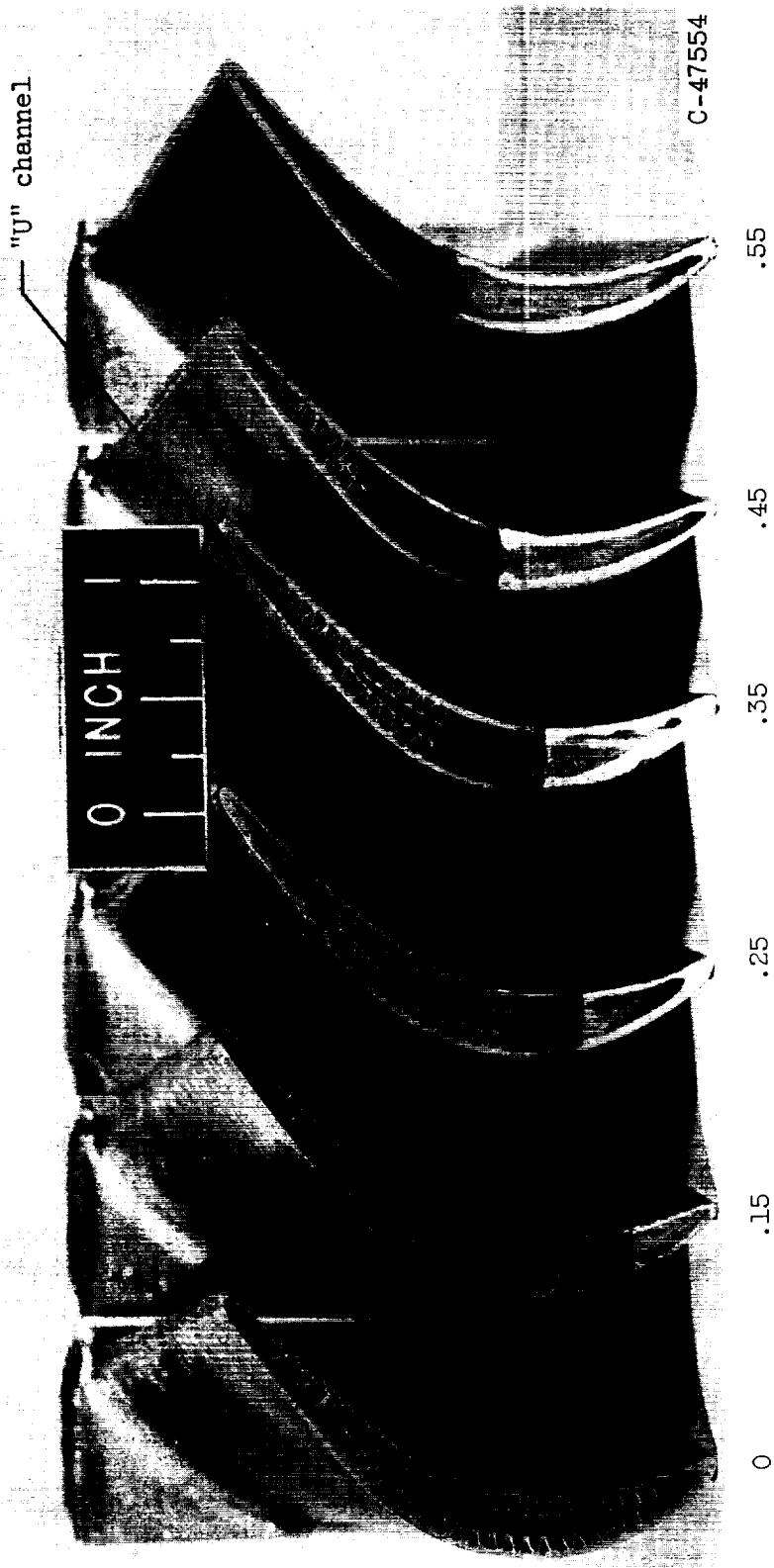
Tip-cap length/Blade chord length

Figure 6. - Leading-edge tip caps on air-cooled turbine rotor blades.

X - Thermocouple

E-1163

Leading edge

Trailing edge

3.69"

1.25"

CD-7225
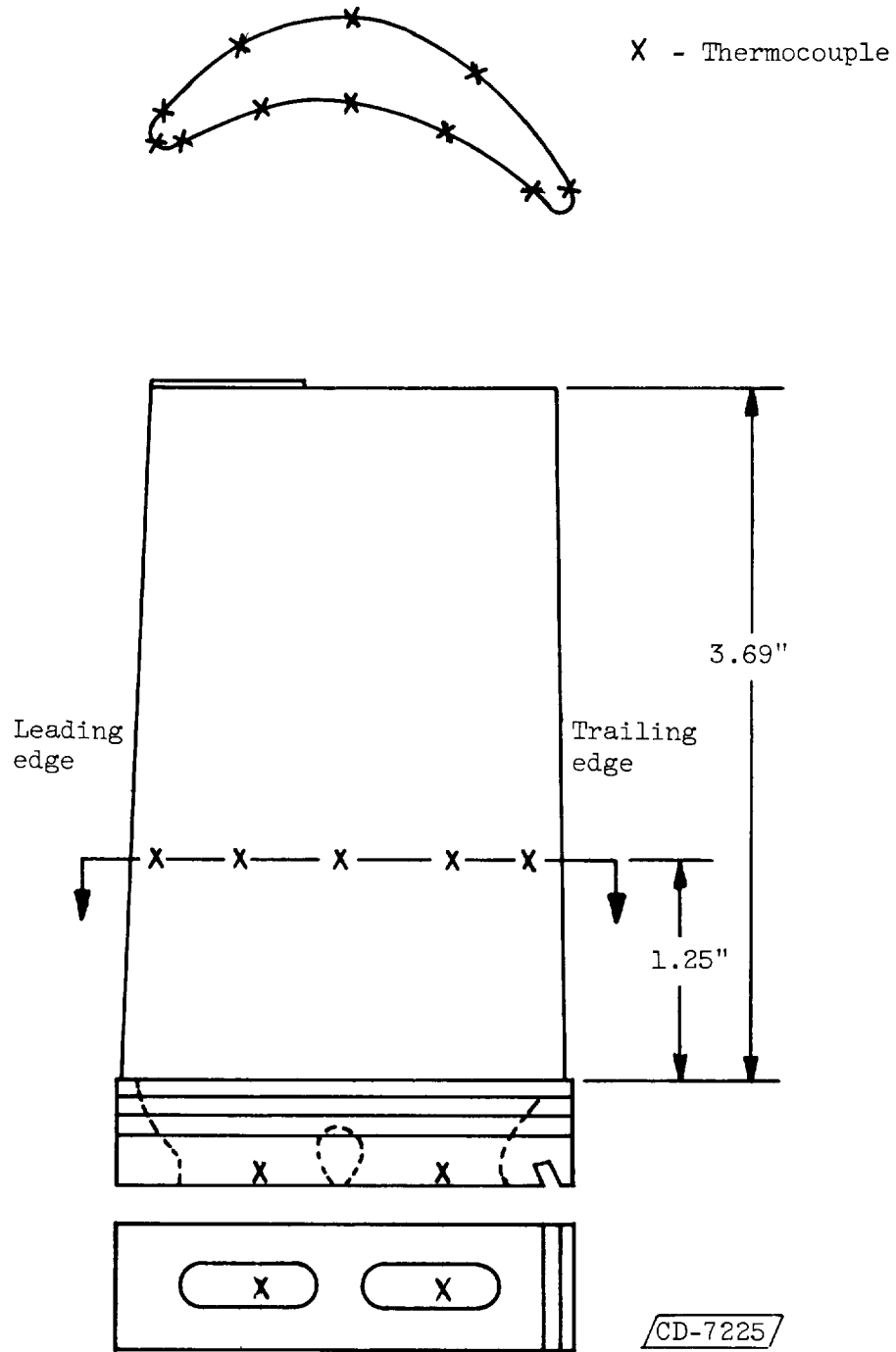
Figure 7. - Thermocouple locations on turbine rotor blade.

	Run	T_3, °F	$t_{g,e}$, °F	t_a, °F	w_a/w_g
——○——	10	2017	1835	91	0.054
——□——	11	2014	1833	120	.039
——◇——	12	2023	1840	183	.024
——△——	13	2012	1830	294	.013
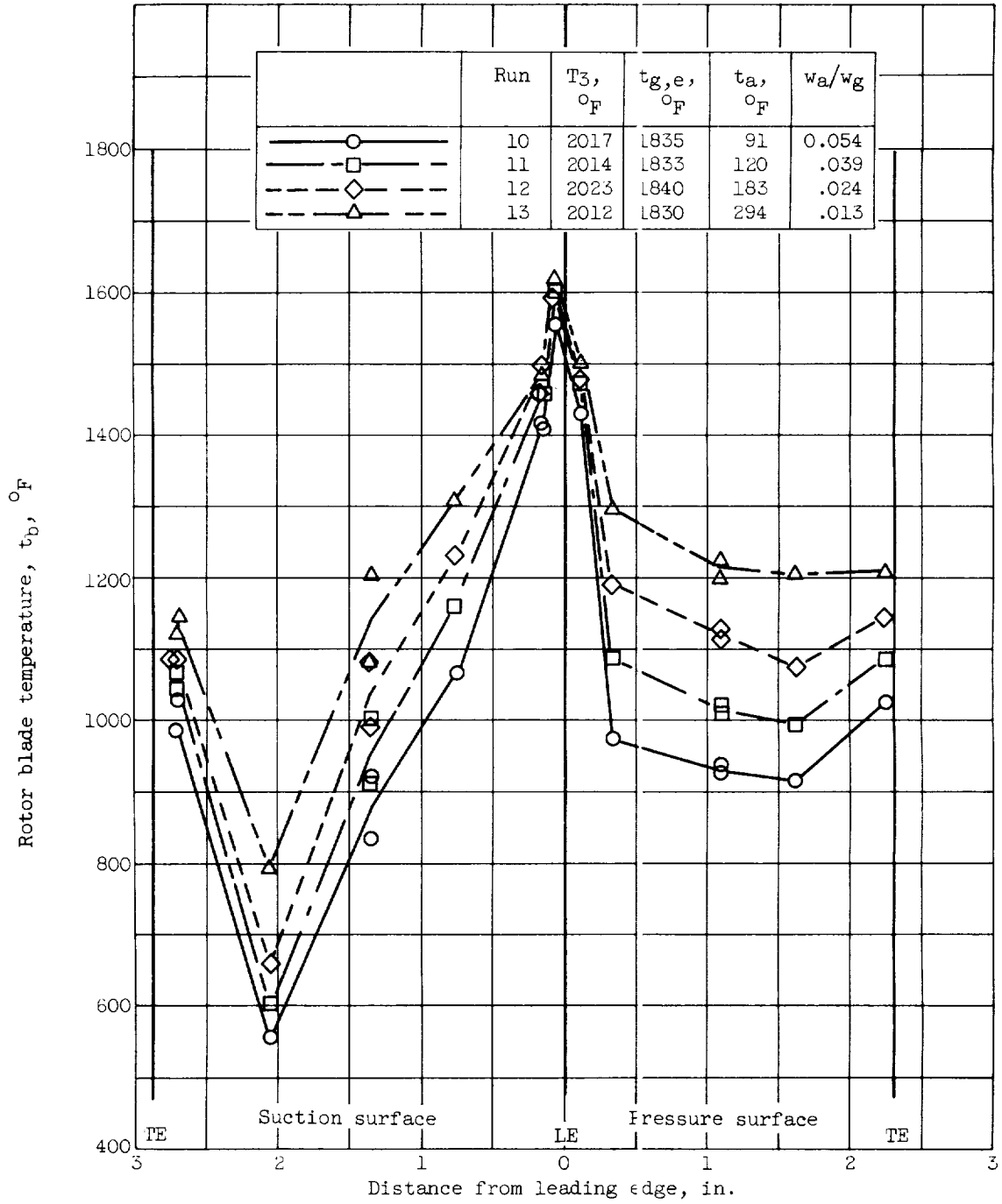
Figure 8. - Chordwise temperature distribution at one-third span of turbine rotor blades with tip caps equal to 35-percent chord. Engine speed, 6970 rpm.

E-1163
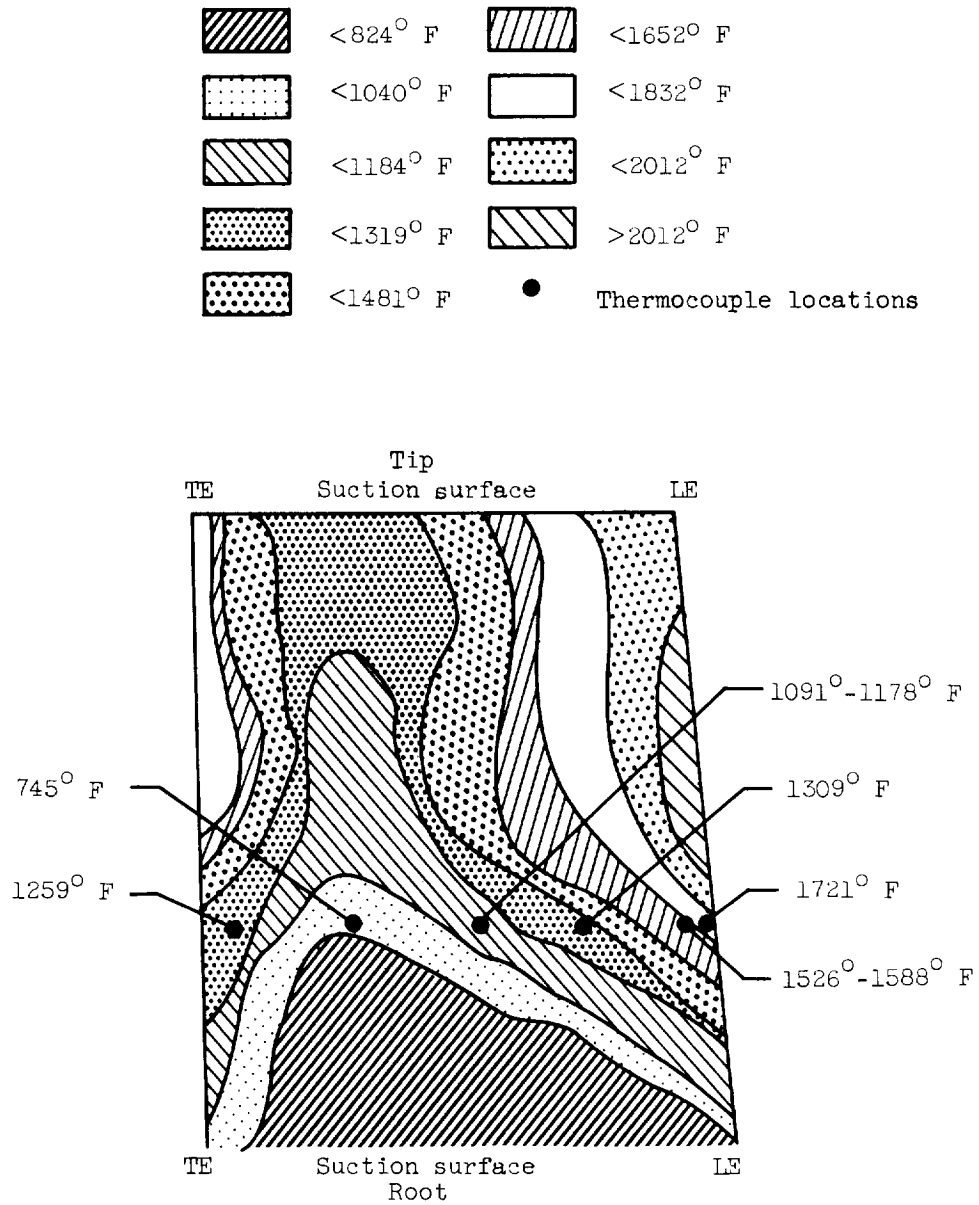
Figure 9. - Composite of thermocouple and temperature-indicating-paint data for suction surface of turbine rotor blades with 0.35-chord tip caps (series E, table I).

(a) Leading edge.

Run	P_a, in. Hg abs	$(w_a/w_g)_{av}$
10	54.5	0.054
11	44.8	.039
12	37.5	.024
13	33.0	.013

$\dfrac{\text{Tip-cap length}}{\text{Chord length}}$

O	0
△	.25
◇	.35
▢	.55
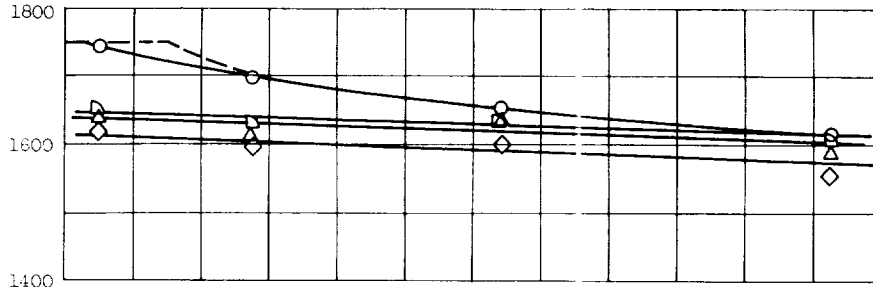
Blade temperature, t_b, °F
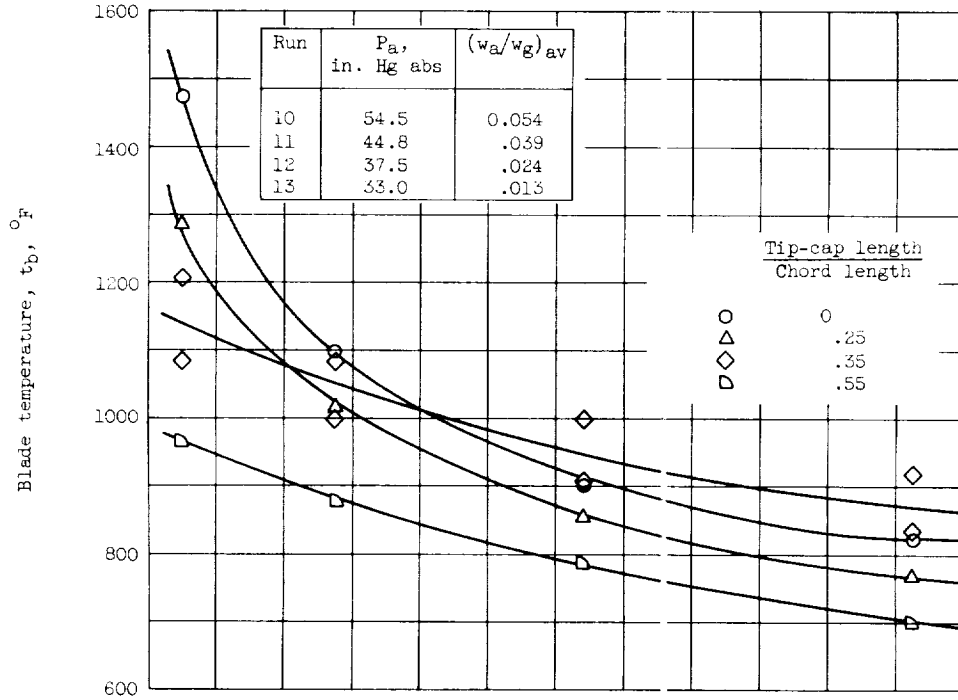
(b) Midchord (suction surface).

(c) Trailing edge.

Rotor hub cooling-air pressure, P_1, in. Hg abs
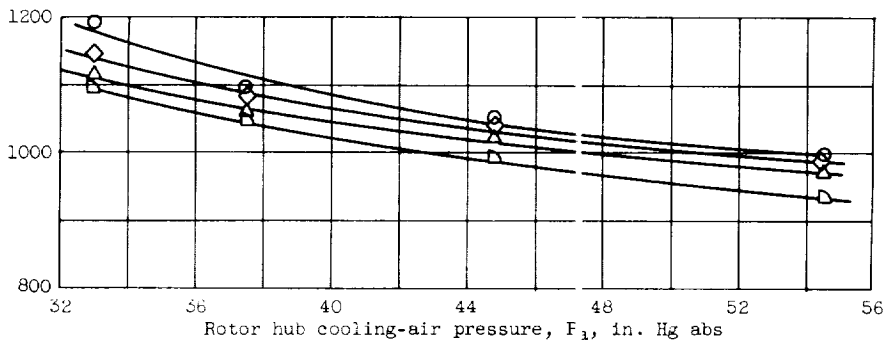
Figure 10. - Local turbine rotor blade temperature at one-third-span position over a range of rotor hub cooling-air pressures (average coolant-flow ratios). Series C (table I); engine speed, 6970 rpm; effective gas temperature, 1743° F.

E-1163
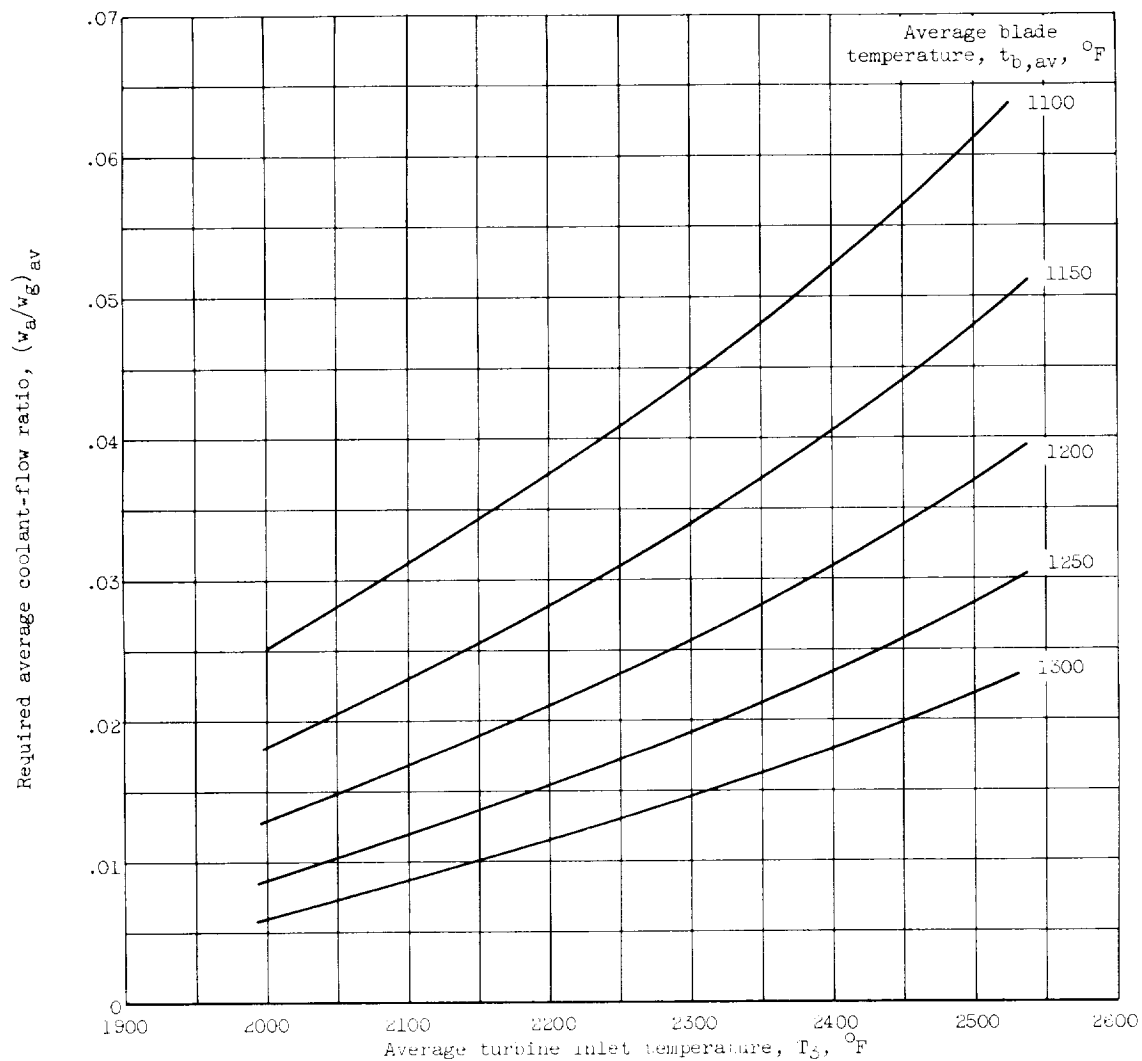
Figure 11. - Required average coolant-flow ratios for various average blade temperatures over range of average turbine inlet temperatures for blade with 0.35-chord tip cap.
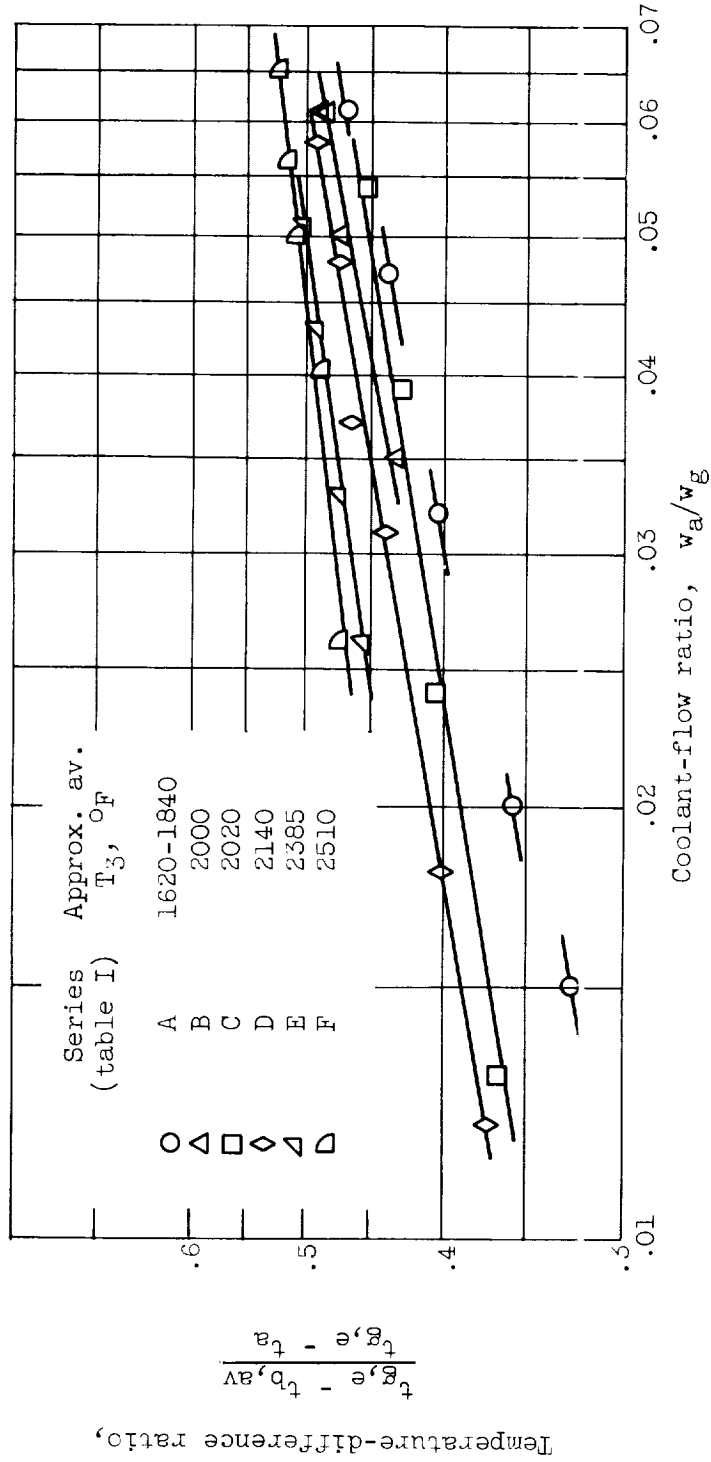
Figure 12. - Variation of temperature-difference ratio with coolant-flow ratio for range of turbine inlet temperatures.
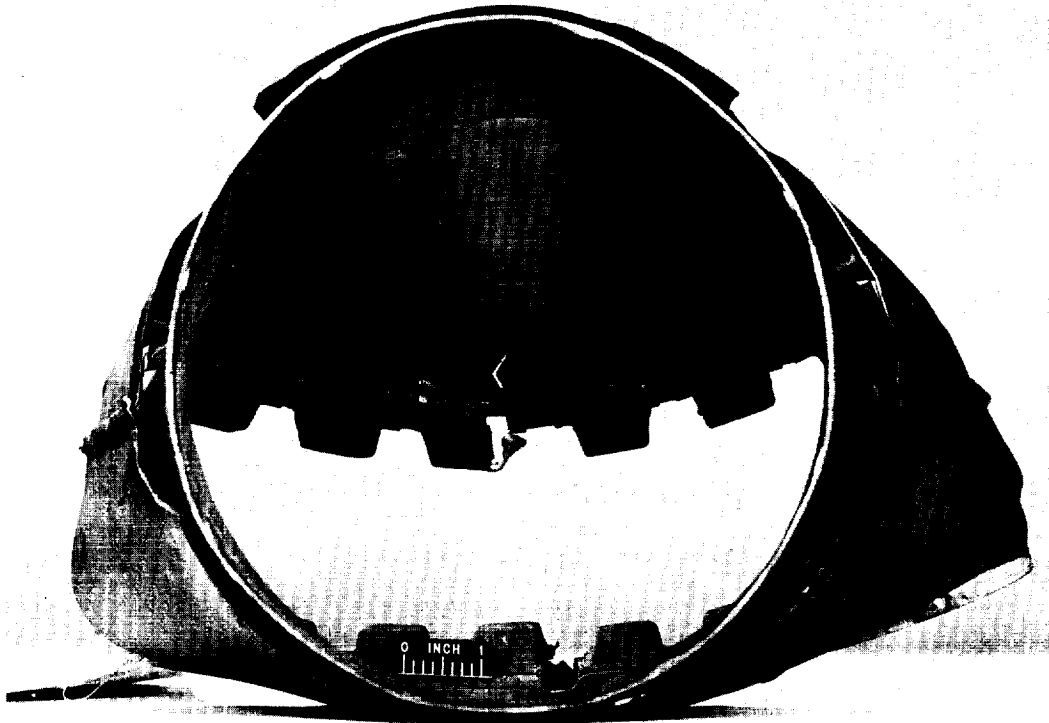
C-53962

(a) Forward view.

Instrumentation cutout
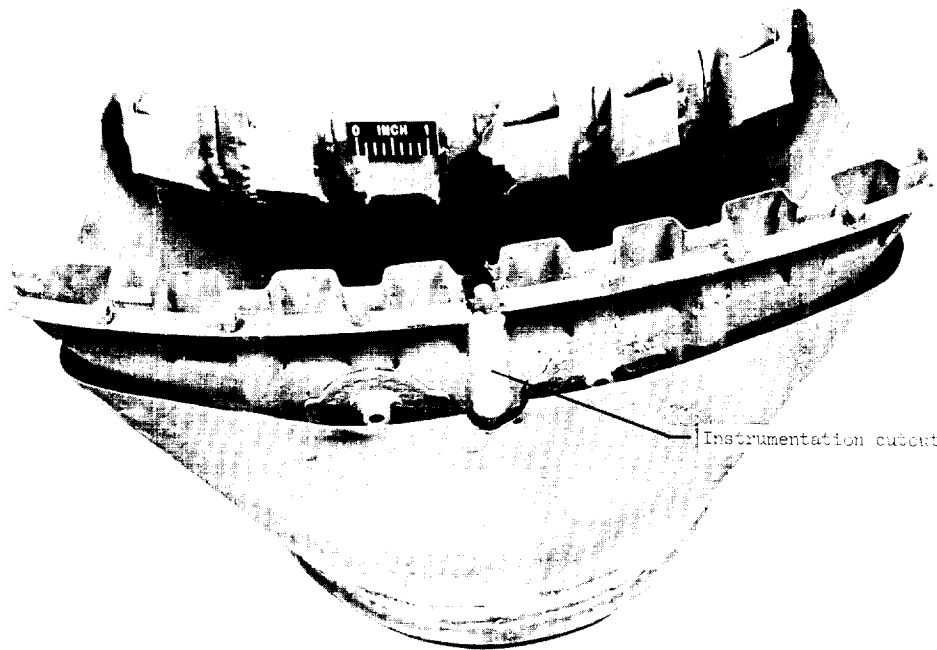
C-53959

(b) Rear view.

Figure 13. - Damage to transition liner due to high-temperature operation.
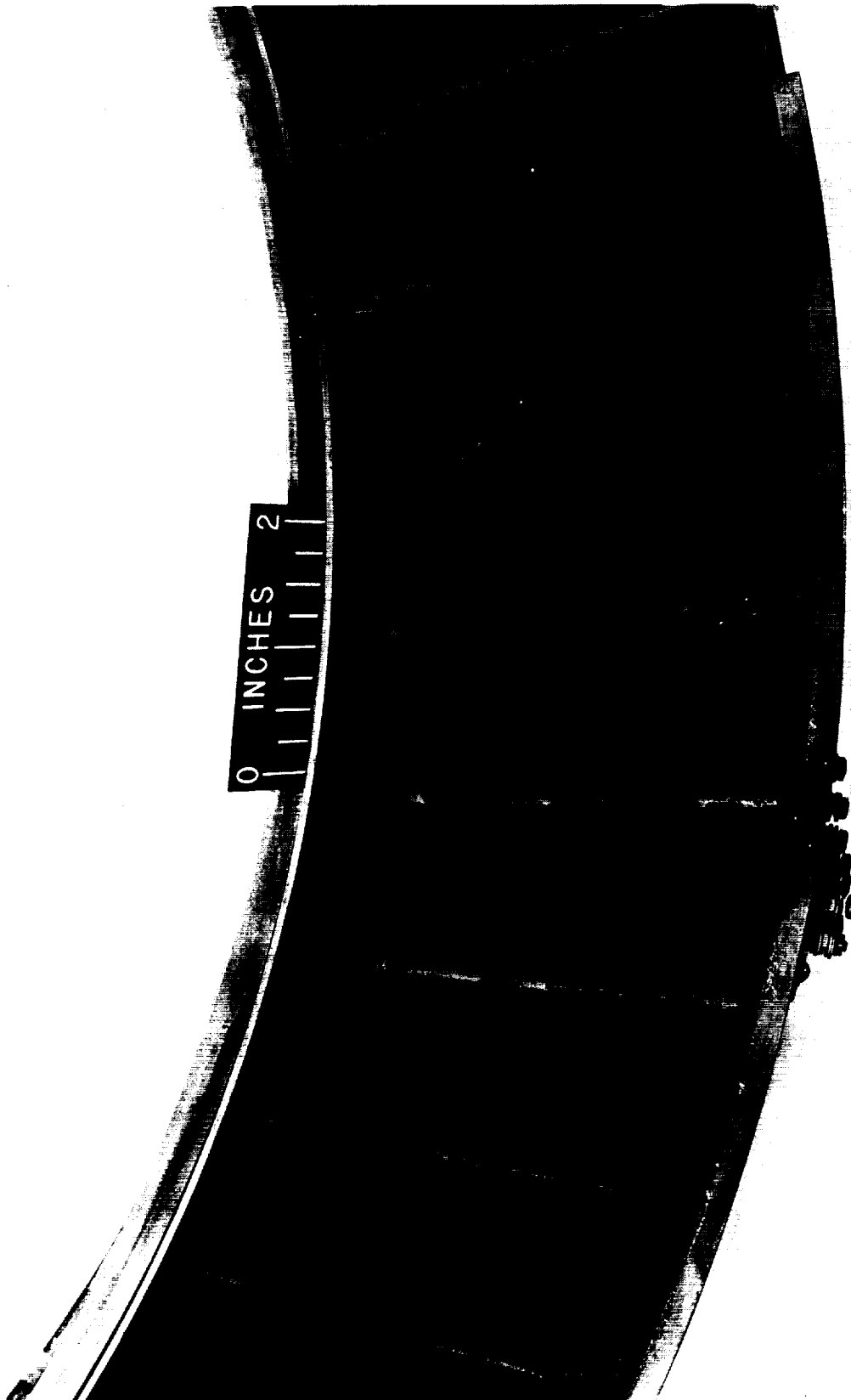
Figure 14. - Typical damage to leading edge of stator blades due to high-temperature operation.

C-53958

E-1163
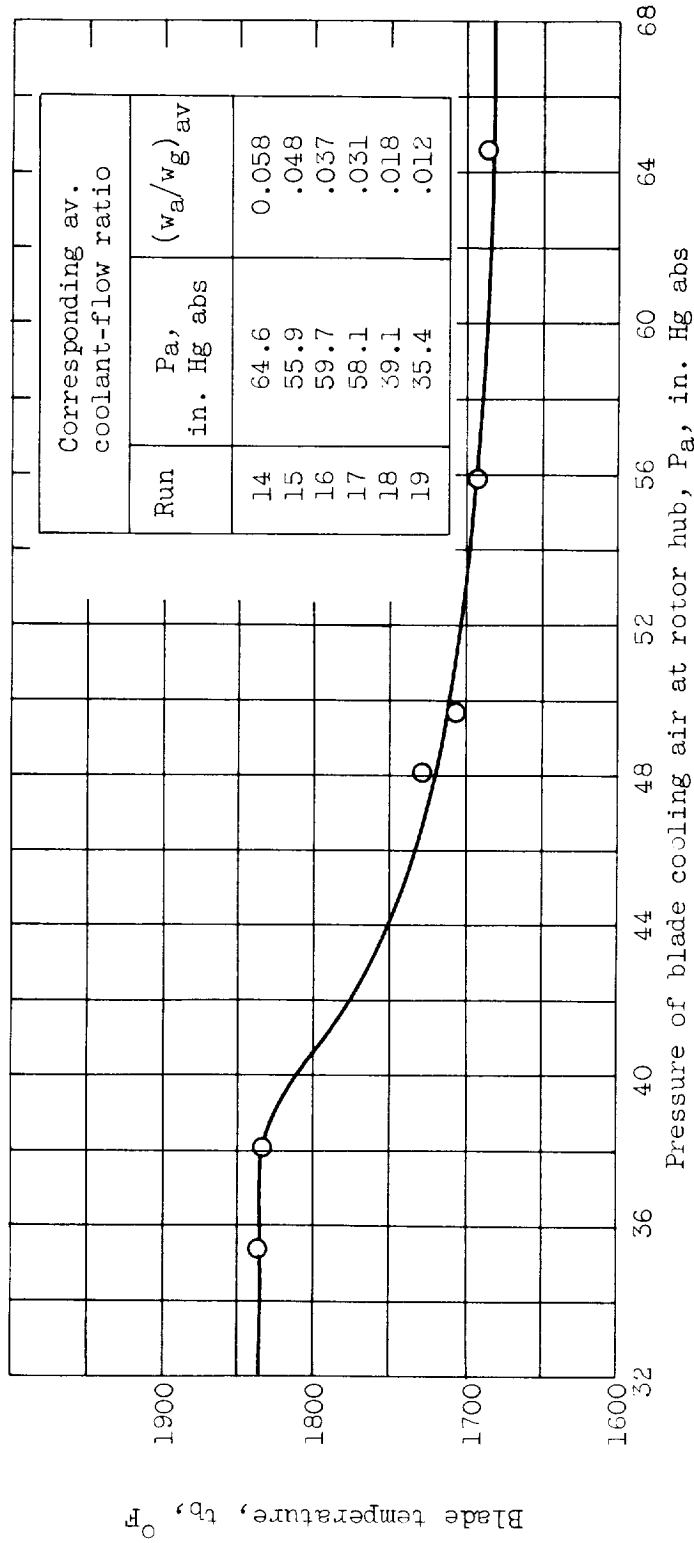
Figure 15. - Variation of uncapped-blade leading-edge temperature with cooling-air pressure for series D engine operation. Engine speed, 7640 rpm; turbine inlet total temperature, 2145° F.